OPTIMAL SIZING OF SYNCHRONOUS CONDENSERS TO IMPROVE SYSTEM STRENGTH UNDER HIGH WIND POWER PENETRATION IN A POWER GRID

by

Sajjad Uddin Mahmud
(0416062104)

Submitted in partial fulfillment of the requirements of the degree of
Master of Science in Electrical and Electronic Engineering

BANGLADESH UNIVERSITY OF ENGINEERING AND TECHNOLOGY
DHAKA-1000, BANGLADESH
August 2020

OPTIMAL SIZING OF SYNCHRONOUS CONDENSERS TO IMPROVE SYSTEM STRENGTH UNDER HIGH WIND POWER PENETRATION IN A POWER GRID

by

Sajjad Uddin Mahmud

(0416062104)

Submitted in partial fulfillment of the requirements of the degree of

Master of Science in Electrical and Electronic Engineering

Under the supervision of

Dr. Nahid-Al-Masood

Associate Professor

Department of Electrical and Electronic Engineering

Bangladesh University of Engineering and Technology (BUET)

BANGLADESH UNIVERSITY OF ENGINEERING AND TECHNOLOGY

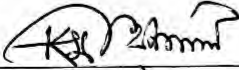DHAKA-1000, BANGLADESH

August 2020

CERTIFICATION OF THESIS

The thesis titled "**OPTIMAL SIZING OF SYNCHRONOUS CONDENSERS TO IMPROVE SYSTEM STRENGTH UNDER HIGH WIND POWER PENETRATION IN A POWER GRID**" submitted by **Sajjad Uddin Mahmud**, Student ID: 0416062104, Session: April/2016 has been accepted as satisfactory in partial fulfillment of the requirement for the degree of Master of Science (M.Sc.) in Electrical and Electronic Engineering on 25 August,2020.
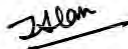
BOARD OF EXAMINERS

Dr. Nahid-Al-Masood
Associate Professor
Department of Electrical and Electronic Engineering
Bangladesh University of Engineering and Technology, Dhaka, Bangladesh

Chairman
(Supervisor)

Dr. Md. Kamrul Hasan
Professor & Head
Department of Electrical and Electronic Engineering,
Bangladesh University of Engineering and Technology, Dhaka, Bangladesh
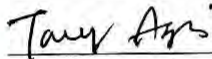
Member
(Ex- officio)

Dr. Mohammad Jahangir Alam
Professor
Department of Electrical and Electronic Engineering
Bangladesh University of Engineering and Technology, Dhaka, Bangladesh

Member

Dr. Md. Shamim Reza
Professor
Department of Electrical and ElectronicEngineering
Bangladesh University of Engineering and Technology, Dhaka, Bangladesh

Member

Dr. Tareq Aziz
Professor
Department of Electrical and Electronic Engineering
Ahsanullah University of Science and Technology, Dhaka, Bangladesh

Member
(External)

Candidate's Declaration

I, Sajjad Uddin Mahmud, declare that this thesis titled, "OPTIMAL SIZING OF SYNCHRONOUS CONDENSERS TO IMPROVE SYSTEM STRENGTH UNDER HIGH WIND POWER PENETRATION IN A POWER GRID" and the work presented in it are fully my own in partial fulfillment of the requirement for the degree of Master of Science (M.Sc.) in Electrical and Electronic Engineering. I confirm that this research work has not been submitted elsewhere for the award of any degree or diploma excepting for publication. Others' works that have been quoted are clearly attributed with source.

_____

Sajjad Uddin Mahmud

Acknowledgement

All praise goes to the Most Gracious and Most Merciful Almighty ALLAH for enabling the author to complete this work.

I would like to express my deepest sense of gratitude to my supervisor, Dr. Nahid-Al-Masood sir, Associate Professor, Department of Electrical and Electronic Engineering, Bangladesh University of Engineering and Technology (BUET), Dhaka, for his kind supervision of this work. His undaunted guidance, untiring efforts, great patience, valuable advices and constant assistance extensively helped me to complete this work. He is my not only my supervisor but also true mentor who will be a significant inspiration to me for rest of my life. Thank you very much Dr. Masood.

Finally, I would like to thank my parents, my sister, my friends and my all well-wishers for the support they have provided me with throughout this challenging time.

Abstract

Wind is one of the most economically viable renewable energy sources and hence, its large scale integration is rapidly increasing in many countries. With increasing wind power, conventional fossil fuel based synchronous generators are being replaced from generation fleet. In recent times, wind power plants are mostly based on type 3 (Doubly-Fed Induction Generator: DFIG) and type 4 (Full Scale Converter: FSC) machines. These variable speed wind turbine generators (WTGs) are decoupled from the corresponding grid by power electronics inverters. Due to constrained capacities of these inverters, type 3 and type 4 WTGs usually generate less fault current compared to synchronous generators. As a result, system strength deteriorates under high penetration of wind power. System strength at the Point of Common Coupling (PCC) of a wind power plant is specified by an index called Short-Circuit Ratio (SCR). A minimum value of SCR is essential for fault identification and successful ride through of wind power plants during faults. To improve system strength, synchronous condensers can be utilized because these devices contribute to fault levels. Since the installation of synchronous condensers is expensive, the optimal strategy to allocate them is of major concern. A number of research works have been reported in the literature on the deployment of synchronous condensers to enhance SCR in wind prolific power systems. The existing methods mainly focus on the optimal location of synchronous condensers to maintain satisfactory SCR. However, these techniques do not provide any optimal sizing of synchronous condensers while considering their installation, operational and maintenance costs. Therefore, further investigations are still required to meet this important yet unaddressed research gap.

In the above perspective, optimal sizing of synchronous condensers to improve system strength in a wind dominated power grid is determined by considering long-term techno-economic viability. Also, the impact of the selected synchronous condensers on system strength during substantial penetration of wind power in a test network is explored. The outcome of this thesis provides useful guidelines for network operators to maintain adequate system strength under high wind penetration by ensuring long-term technical as well as financial benefits.

Table of Contents

List of Figures

List of Tables

List of Abbreviations

DFIG	Doubly-Fed Induction Generator
DG	Diesel Generator
FSC	Full-Size Converter
GE	General Electric
GW	Gigawatt
GWh	Gigawatt-hour
Hz	Hertz
MVA	MegaVolt-ampere
MW	Megawatt
MWh	Megawatt-hour
NEM	National Electricity Market
NSC	New synchronous condenser
OF	Objective function
p.u.	Per unit
PCC	Point of common coupling
PRS	Post-retirement scheme
PSS®E	Power System Simulator for Engineering
ROCOF	Rate of change of frequency
SCC	Short-circuit capacity
SCR	Short-circuit ratio
VA	Volt-ampere
WPL	Wind penetration level
WTG	Wind turbine generator

List of Symbols

S''^{i}_{k}	Initial symmetrical short-circuit apparent power at bus i
P^{i}_{max}	Rated power of the wind farm link to PCC i
I''^{i}_{k}	Initial symmetrical short-circuit current
V^{i}_{n}	Rated voltage at bus i
Z^{i}_{k}	Thevenin equivalent short-circuit impedance
R_i	Net revenues during the i-th year
C_i	Net costs during the i-th year
C_0	Installation cost of synchronous condensers
SCR_{min}	Minimum short-circuit current
N_{PCC}	Number of point of common coupling
C_f	Fixed cost per synchronous condenser installed
C_v	Variable cost per MVA installed
$S(x)$	Function that indicate the rating/size (x) of synchronous condenser installed at a wind plant PCC
C_{mavg}	Averaged maintenance cost per MVA per year
$C_{main}(x)$	Maintenance cost of synchronous condenser of size x per year
$C_{elec}(x)$	Total cost of electricity
P_{loss}	Internal loss of synchronous condenser
R_{wtg}	Yearly revenue obtained by additional electricity generated and sold
R_{fuel}	Yearly fuel saving
α	Wind curtailment reduction factor
C_{MWH}	Yearly averaged cost of electricity

Chapter 1
Introduction

1.1 Background

Climate change is progressing at an alarming rate and fighting against it is a challenging task to make sure the next generation will find life on this earth worth living. Through its high CO_2 abatement potential, wind energy can help to stop global warming. It is not only the most sustainable but also the most economical source of energy [1]. Energy security, diversity of electricity supply and low carbon emissions have been major drivers in recent large-scale wind energy developments around the world. It has been projected that wind power would supply more than one-third of total electricity demand by 2050 as shown in Figure 1.1. Note that it is well aligned with energy transformation scenarios of various institutions, clearly highlighting the importance of scaling up the wind power generation share in order to decarbonize the energy system in the next three decades [2].
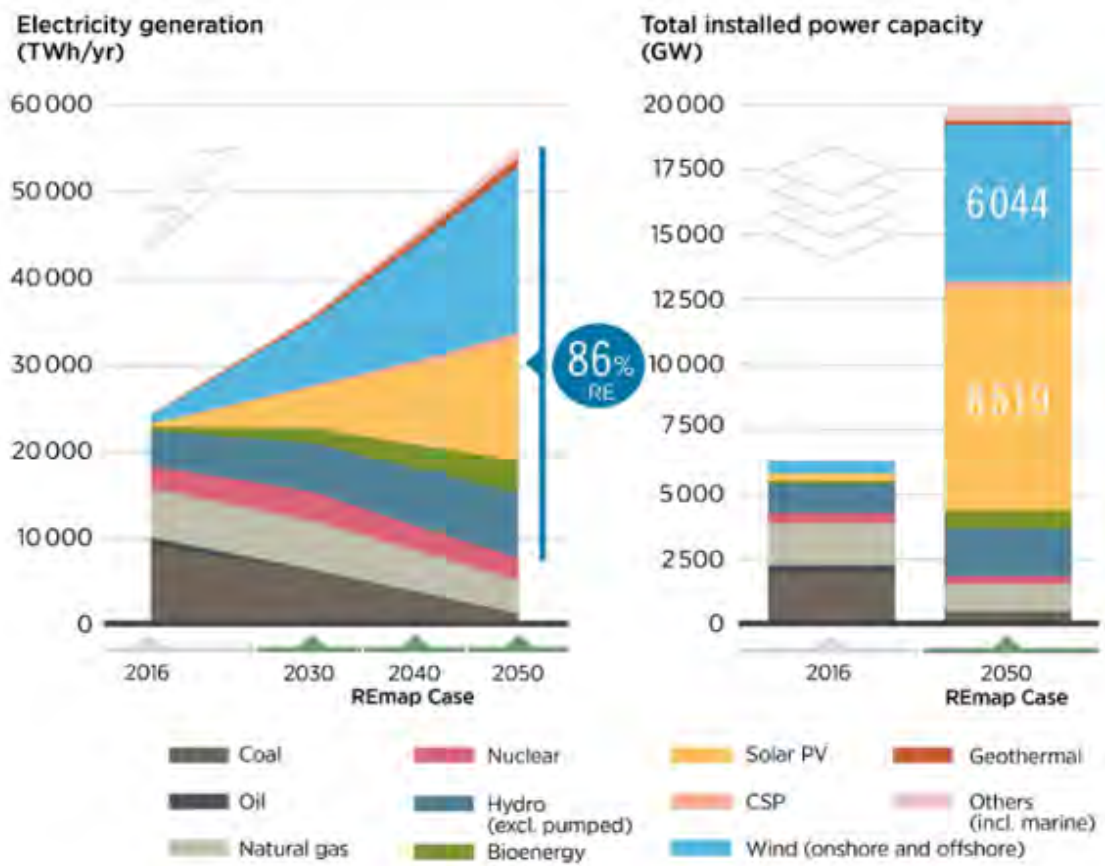
Figure 1.1: Wind would be the largest generating source, supplying more than one-third of total electricity generation needs by 2050 [2].

The total installed capacity for onshore and offshore wind energy globally is over 651 GW by the end of 2019 [1]. The proliferation of wind power generation capacity around the world in the last decade is shown in Figure 1.2.
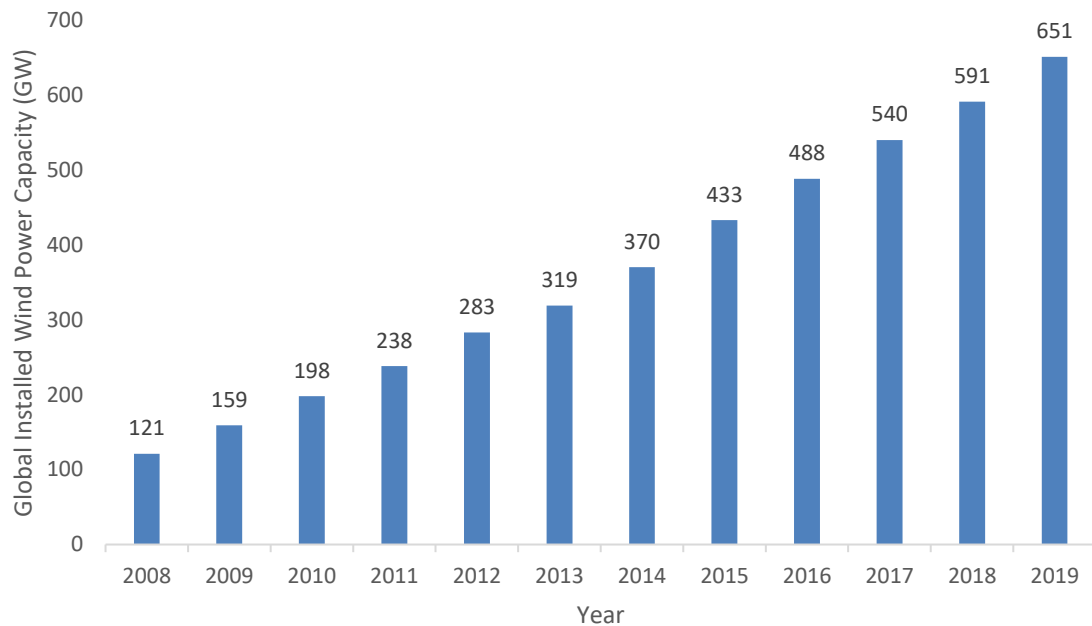
Figure 1.2: Growth of global installed wind generation capacity [1].

Wind power plant converts the kinetic energy of wind into electrical energy by using a large wind turbine consisting of blades on a shaft. When wind flows through the turbine, it moves the blades that eventually rotate the shaft. The shaft is connected to a generator. Its spinning motion is used to rotate the generator's rotor. By creating electromagnetic induction from that rotational movement of the rotor inside the generator core, electrical energy is produced.

Wind turbine generators (WTGs) can be divided into four main types [3, 4, 5]:

    i.   Type-1 (Fixed Speed Induction Generator): It uses a squirrel-cage induction generator.

    ii.   Type-2 (Variable-Slip Induction Generator): It utilizes a wound-rotor induction generator.

    iii.   Type-3 (Doubly-Fed Induction Generator: DFIG): It is a variable speed machine where an induction generator and power electronic converters are utilized.

    iv.   Type-4 (Full-Size Converter: FSC machines): It is akin to Type 3 WTG but the generator can be an induction generator or a synchronous generator.

Nowadays, the most common types of wind generator are Type-3 and Type-4 WTGs because of their cost effectiveness and higher efficiency [4, 6]. Due to power electronic

converters, Type-3 and Type-4 WTGs are decoupled from the corresponding grid [7]. Therefore, these machines cannot behave like the conventional synchronous generator of equivalent rating. In other words, these machines are non-dispatch able and have limited fault current contribution and frequency control capability.

While wind energy offers several advantages from environmental aspects, it also causes technical challenges for system operation [8]. The important operational metrics that are affected by increased wind penetration are mostly related to-

     i.   Frequency response

    ii.   Short-circuit performance (also known as system strength)

   iii.   Voltage stability

   iv.   Harmonic distortion and

    v.   Variability, uncertainty, and reliability

System strength indicates the capability of a power system to recover a fault. Among the aforementioned operational metrics, satisfactory system strength is one of the major challenges regarding power system security under high penetration of wind generation.

1.2 Motivation of this study

Wind power integration in power grids causes replacement and retirement of synchronous generators from generation fleet, which tends to reduce system strength. As such, a predefined number of synchronous generators are deliberately kept online to ensure adequate system strength in wind dominated power systems. It results in the curtailment of wind power which eventually causes financial concerns. To mitigate this issue, synchronous condensers can be a worthwhile choice since these devices contribute to fault level to enhance system strength. However, utilization of synchronous condensers needs further investigations. The existing research works mainly focus on the optimal location of synchronous condensers. Nevertheless, those works did not take the optimal sizing of the synchronous condensers in consideration which is the focal point of this thesis.

1.3 Objectives

The principal goal of this thesis is to comprehensively analyze the short-circuit strength under substantial wind penetration in a power system. A necessary technique to enhance this security index is also developed. The specific objectives of this work are as follows:

i. To investigate the system strength (i.e. short-circuit performance) at the PCC of wind power plants under high wind power penetration in a power grid.

ii. To determine the optimal sizing of synchronous condensers to improve system strength in a wind dominated power grid by considering long-term financial viability.

iii. To analyze the impact of the selected synchronous condensers on system strength during substantial penetration of wind power.

The possible outcome of this thesis will suggest the most appropriate sizing of synchronous condensers to enhance system strength during high wind power penetration in a power grid. Therefore, this work will enable large-scale integration of wind power while taking into account the techno-economic benefits for network operators.

1.4 Thesis Layout

This thesis consists of five chapters. The structure of the thesis is as follows:

- In Chapter 1, a brief description of current and future global wind energy scenario is described. Then, motivation of the current work is presented along with the objectives.

- In Chapter 2, a thorough review of relevant work is narrated. Then, the research gaps are identified.

- In the beginning of Chapter 3, the impact of high wind penetration on system strength is explored. To this end, load flow study and evaluation of system strength are described at first. Next, a test power system network is presented that is utilized for further investigations. Furthermore, the implication of synchronous condensers on system strength is explored.

- In Chapter 4, an algorithm is presented to determine the optimal sizing of synchronous condensers to maintain adequate system strength under high wind power penetration. In addition, the proposed algorithm is validated by comparing its techno-economic benefits with that of an existing approach.

- Finally, in Chapter 5, the key findings are summarized and the possibilities of future research work are mentioned.

Chapter 2
Literature Review

In this chapter, at first the worldwide scenario of wind power is briefly discussed. Afterwards, the major challenges caused by higher wind power penetration are shortly described. Then, a comprehensive literature review on power system security issues especially short-circuit performances are presented.

2.1 Wind Power Scenario Worldwide

Wind power has now established itself as a mainstream electricity generation source and plays a significant role in number of countries' energy plans. According to the latest statistics, the total installed electricity generation capacity from wind across the world is around 650.8 GW in which 59.7 GW was added in 2019 [9]. At present, China has the highest installed wind power capacity, a total of 273.03 GW. Furthermore, the U.S., Germany, India, Spain, the U.K., France and Brazil are the leading countries with remarkable wind generation capacities [10]. However, in Bangladesh, the total installed wind power capacity is 2.9 MW till 2020 [11]. The top ten countries in terms of installed capacity of wind power are shown in Figure 2.1.
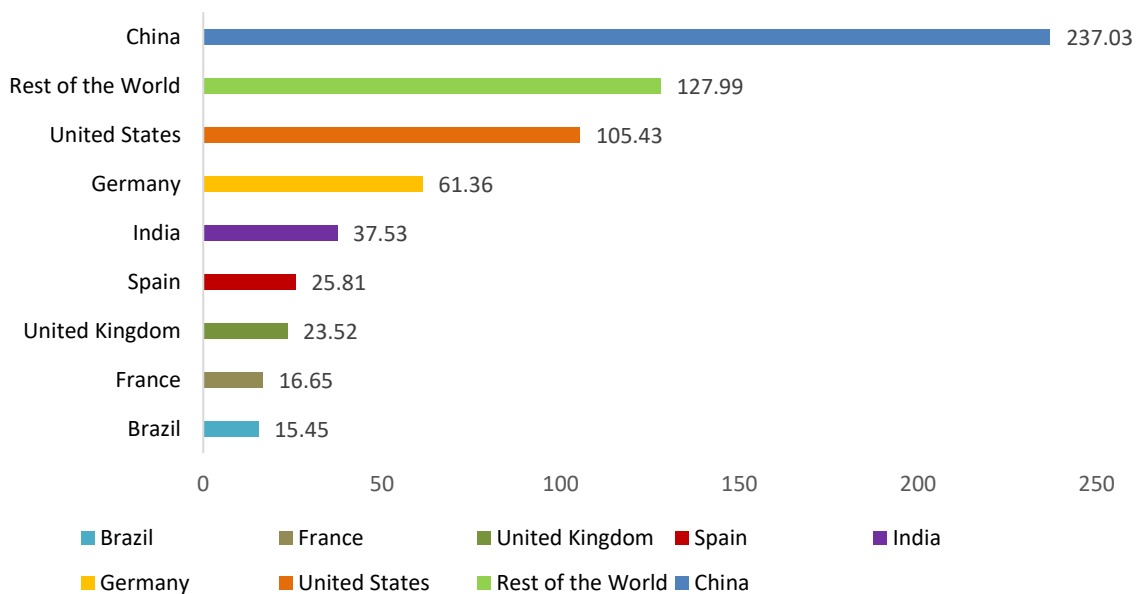
Figure 2.1: Installed wind generation capacity in various countries [10].

Although wind energy brings several benefits to power systems, it also introduces a number of technical challenges related to network operation [12]. In the next sub-section, some important issues instigated by high wind penetration are highlighted.

2.2 Challenges due to High Wind Power Penetration

The secured operation of a power system is regarded as the ability to withstand disturbances without causing a failure of the power system [13]. Wind power generation often introduces a number of challenges in terms of security, stability and reliability the power grid. These issues become more prominent during prolific wind penetration levels [14, 15]. The key challenges arising from higher wind power penetration are broadly discussed below.

2.2.1 Frequency Response

Frequency control is a vital aspect of system integrity in power grid. The grid frequency must be maintained within a compact range around its nominal value all the time. A contingency can cause sudden decline in grid frequency. This sudden change must be mitigated as soon as possible with proper control action. Conventional synchronous generators (SGs) usually have large rotating masses that can create sufficient inertia. The kinetic energy that stored in the rotor of SGs, is spontaneously used for the dynamic power balance to maintain grid frequency following a loss of generation [16].

Most new wind power plants are constructed based on Type 3 and Type 4 wind machines, which are connected to the grid through power electronic devices. These make the WTG asynchronous in nature. Therefore, these WTG are unable to provide inertia effect (instantaneous reaction to counteract the sudden change in frequency) as well as governor function to help restore frequency [13, 17, 18]. Moreover, nowadays, WTG are replacing traditional synchronous generator from the generator fleet. This increasing penetration of nonsynchronous sources causes the maximum frequency deviation and rate of change of frequency (ROCOF) more extreme following a large contingency [19].

For frequency response, several control strategies for Type 3 and Type 4 WTGs have been developed [20, 21]. In addition, an approach called Post-Retirement Scheme (PRS) has been developed in [22], which proposes to re-use the retired synchronous generator to improve frequency response.

2.2.2 Short-Circuit Level

Short-circuit level or fault level is the amount of current or volt-ampere (VA) that feeds into a fault at a given point in a power system [23]. When a fault occurs, protection devices are meant to operate rapidly and selectively in order to quickly isolate the faulted elements from the network. This is essential for power system network security and stability. During fault, a much higher current compared to normal operating condition is initiated. Protection devices intend to identify that a fault has occurred. Therefore, power system protection devices are designed to take into account the maximum and minimum short-circuit levels. The fault current depends on the generators, which are committed at the time of a fault occurrence. If a number of generators operate near a fault point, the short-circuit level will be higher. On the other hand, the short-circuit level will be lower when no/ fewer generators are committed near a fault location.

Fault calculations under various operating conditions are performed by a system operator for the following purposes.

- To correctly identify faults.
- To select proper ratings of a circuit breaker. The breaker should be able to identify a fault and interrupt the maximum possible fault current at a specific point in a network.
- To design a coordinated protection system.
- To accomplish the mechanical design of network components, which should survive the high mechanical stress during a fault.

As modern WTGs displace the conventional synchronous generators, the short-circuit strength of a grid may become a concern. These modern Type 3 and Type 4 WTGs usually generate less fault current compared to synchronous generators of equal rating [24, 25, 26].

SCR is a performance index, which is used to specify the strength of a grid at the PCC. SCR is defined as the ratio between short-circuit level and rated generation capacity of a wind farm at its PCC. A minimum value of SCR (3 to 5) is required for WTGs to ensure successful fault ride through as well as re-establishment of stable operation of the WTGs after the fault is cleared [22, 27].

Low SCR could result in practical power system problems related to fault identification. Protective devices detect a fault based on the minimum short-circuit current, which is around 3 to 5 times of the rated current. If the magnitude of the fault current is less than this minimum threshold, protective devices like relays cannot identify the fault. As a result, the associated circuit breakers do not trip and system continues to feed the fault. This may cause voltage

instability. It is observed that when wind power penetration increases in a power grid, the value of SCR at PCC decreases. SCR under various network conditions of a real-world power system is shown in Figure 2.2.
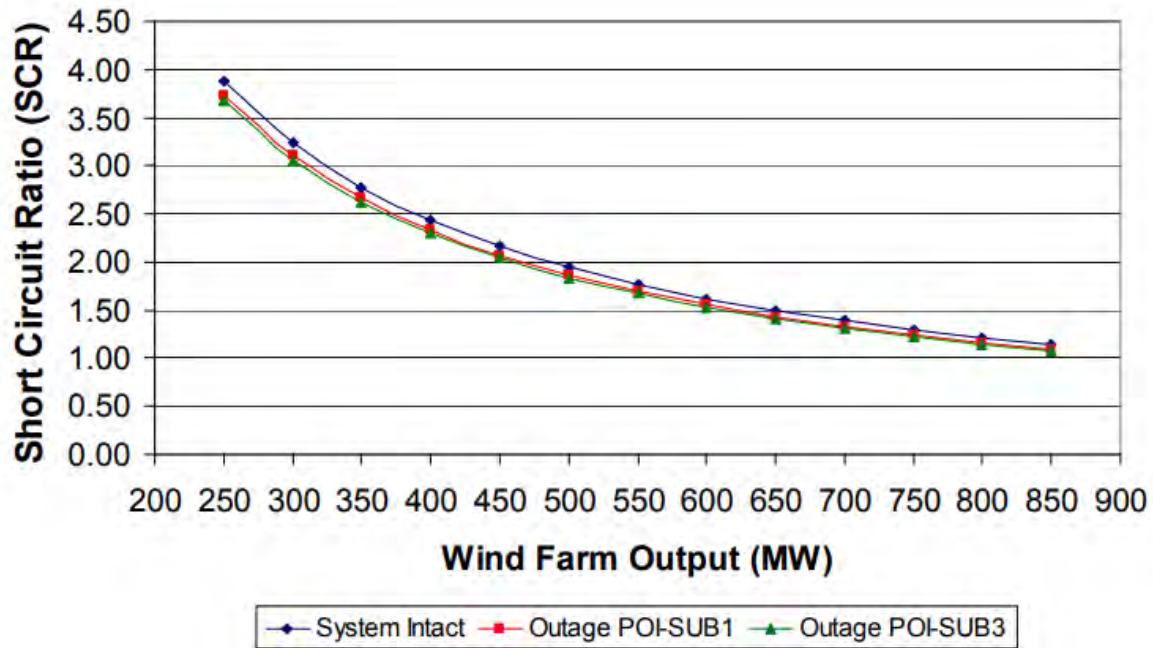
Figure 2.2: Relationship between SCR and wind farm output (capacity) [28]

2.2.3 Voltage Stability

Maintaining the voltage within the operational limit is always considered as one of the critical issues. For instance, the fluctuation of wind power output causes voltage fluctuations and voltage drops that depend on the variation of wind speed and type of generation system. WTGs are mainly divided into fixed-speed and variable-speed induction generators. The fixed speed generators absorb reactive power that relies on the speed of the rotor and thus creates voltage fluctuation in power grids [29]. Though deploying the variable-speed wind turbines can smooth 75% of the voltage fluctuations produced by fixed-speed turbines [30, 31, 32], due to the constrained capacity of the PWM (pulse-width modulation) converter, the voltage regulation capabilities of Type 3 and Type 4 WTGs are less than that of synchronous generators. Thus, wind dominated power grids can face voltage instability.

2.2.4 Harmonic Distortion

Wind turbines with converters inject harmonics into the network during their operation, which may potentially create voltage distortion problems [33]. Design of power electronic

8

converters and filters are the influencing factors of harmonics produced by wind turbines. Several studies have introduced various control mechanism to reduce harmonics produced by WTGs [34, 35]. Besides, the deployment of appropriate energy storage systems and filter can also mitigate the harmonics caused due to the integration of wind power plants [36].

2.2.5 Variability, Uncertainty and Reliability

In wind integrated systems, the output power prediction plays a vital role in reducing cost of production. Moreover, unpredictable events of ramps can reduce the reliability of the grid. Furthermore, for WTGs, forecasting is another major task for network management. However, there is no ideal strategy for the prediction of wind energy. Each methodology has its advantages and disadvantages, which may be reasonable in certain specific cases and inappropriate in different cases [37, 38]. Finally, high penetration of wind power creates a challenge to supply customer demand while maintaining a certain level of reliability.

2.3 Research Gap

Ensuring secured operation of an electric power grid is of utmost importance. There are various symmetrical and unsymmetrical faults that can be occurred in grid. Symmetrical three phase fault is the most severe fault [39]. During a fault, the conventional synchronous generator can provide enough fault current. This fault current is needed for switchgear equipment, electromechanical relays, circuit breakers and other protection devices to start their operation and ensure grid stability.

Due to increasing penetration of wind power plant, existing synchronous generators are being replaced from generation mix. However, modern wind turbines such as Type 3 and Type 4 machines usually do not provide enough fault current during faults due to current saturation limits of converters [24, 40, 41]. Under such situations, the system strength of a power grid may be unacceptably low. To indicate system strength of a power gird, an index called Short-Circuit Ratio (SCR) is widely used. For a grid connected wind power plant, SCR at the Point of Common Coupling (PCC) is defined as the ratio between the short-circuit capacity (i.e. short-circuit VA) at the PCC and the rated capacity of the wind power plant. A minimum value of SCR is essential for fault identification and successful ride through of wind power plants during faults [22, 40, 42]. Therefore, to attain satisfactory dynamic stability and operation of protection devices, the value of SCR should be higher than the minimum value.

To improve system strength, synchronous condensers can be utilized because these machines contribute to fault levels [42, 43]. Since the installation of synchronous condensers is expensive, the optimal strategy to allocate them is of major concern. A number of research works have been reported in the literature on the deployment of synchronous condensers to enhance SCR in wind prolific power systems [41, 42, 22, 43, 44]. The existing methods mainly focus on the optimal location of synchronous condensers to maintain satisfactory SCR. However, these techniques do not provide any optimal sizing of synchronous condensers while considering their installation, operational and maintenance costs. Therefore, further investigations are still required to meet this important yet unaddressed research gap.

<div align="center">

Chapter 3

Assessment of the Impact of High Wind Power Penetration on System Strength

</div>

Before determining the optimal size of synchronous condensers, the impact of high wind penetration on the system strength needs to be comprehensively analyzed. To this end, the necessary concepts regarding load flow and system strength calculation is introduced at first in this chapter. Then, a test network is built in a widely accepted power system simulation platform. Afterwards, system strength is investigated under various wind penetration level. Finally, the effectiveness of synchronous condenser to improve system strength under prolific wind penetration is explored.[1]

3.1 Load Flow Study

For any power system study, the inception point is a well-converged load flow case. The principal information obtained from a load flow or power flow study is the magnitude and phase angle of the voltage at each bus and the real and reactive power flowing in each line [39]. Load flow calculation is done before determining fault current. Convergence of load flow allows to proceed to the next steps of pertinent calculation and analysis. Further modifications are done when any warning is shown after the load flow analysis. There are multiple numerical methods to solve load flow equations in a power system. The basic two ways are:

- Gauss-Seidal method
- Newton-Raphson method

In this study, full Newton-Raphson method is taken into account for load flow analysis considering its wide acceptance is power system studies.

---

[1] This chapter has significant materials from the following article published
- S. Uddin Mahmud, Nahid-Al-Masood and S. Rahman Deeba, "Assessing Impact on System Strength Under High Wind Power Penetration," *2019 IEEE International Conference on Power, Electrical, and Electronics and Industrial Applications (PEEIACON)*, Dhaka, Bangladesh, 2019, pp. 79-82.

3.1.1 Newton-Raphson Method

The Newton-Raphson algorithm is the most commonly used iterative method to solve the power flow problem [45]. When applied to the power flow problem, the Newton-Raphson algorithm is utilized to solve for a vector (x), which consists of bus voltage magnitudes ($|V|$) and angles (δ). It can be shown as follows.

$$x = \begin{bmatrix} \delta \\ |V| \end{bmatrix} \tag{3.1}$$

Note that,

1. The voltage magnitude and angle at the swing bus is specified and is therefore not a part of the solution vector x.
2. Bus voltage magnitudes at PV buses (i.e. generator buses) are specified and therefore not part of $|V|$. Only the bus voltage magnitudes of PQ buses (i.e. load buses) are included.
3. δ includes all PQ and PV buses.

Therefore, the vector x is an $m \times 1$ vector with:

$$m = 2n_{PQ} + n_{PV} \tag{3.2}$$

Where, n_{PQ} = the number of PQ buses and

$\quad\quad n_{PV}$ = the number of PV buses

3.1.1.1 Basic Algorithm

The basic Newton-Raphson iteration is as follows:

$$\begin{bmatrix} \delta_{k+1} \\ |V|_{k+1} \end{bmatrix} = \begin{bmatrix} \delta_k \\ |V|_k \end{bmatrix} - [J]^{-1} \begin{bmatrix} \Delta P_k \\ \Delta Q_k \end{bmatrix} \tag{3.3}$$

Where, $\boldsymbol{\delta}_k$ = vector of bus voltage angles at the k-th iteration

$\quad |V|_k$ = vector of bus voltage magnitudes at the k-th iteration

$\quad \Delta P_k$ = $P_{spec} - P_{calc}(\boldsymbol{\delta}_k, |V|_k)$ = vector of mismatches between the specified and calculated bus real power injections (with calculated injections computed using bus voltage magnitudes and angles at the k-th iteration)

$\quad \Delta Q_k$ = $Q_{spec} - Q_{calc}(\boldsymbol{\delta}_k, |V|_k)$ = vector of mismatches between the specified and calculated bus reactive power injections (with calculated injections computed using bus voltage magnitudes and angles at the k-th iteration)

$\quad [J]$ = Jacobian matrix

3.1.1.2 Jacobian Matrix

By convention, the Jacobian matrix is set up as a partitioned matrix of the form:

$$[J] = \begin{bmatrix} \dfrac{\partial P}{\partial \delta} & \dfrac{\partial P}{\partial V} \\ \dfrac{\partial Q}{\partial \delta} & \dfrac{\partial Q}{\partial V} \end{bmatrix}$$

Where each term is a sub-matrix of the form (using $\dfrac{\partial P}{\partial \delta}$ as an example):

$$\frac{\partial P}{\partial \delta} = \begin{bmatrix} \dfrac{\partial P_i}{\partial \delta_1} & \cdots & \dfrac{\partial P_1}{\partial \delta_n} \\ \vdots & \ddots & \vdots \\ \dfrac{\partial P_m}{\partial \delta_1} & \cdots & \dfrac{\partial P_m}{\partial \delta_n} \end{bmatrix} \tag{3.4}$$

In rectangular form, the terms in the sub-matrices are real numbers, which are calculated by the following expressions:

i.   **Sub-matrix $\dfrac{\partial P}{\partial \delta}$:**

$$\frac{\partial P_i}{\partial \delta_i} = \sum_{k=1, k \neq i}^{n} |V_i|\, |V_k|[B_{ik} \cos(\delta_i - \delta_k) - G_{ik} \sin(\delta_i - \delta_k)]$$

$$= -Q_i - B_{ii}V_i^2 \tag{3.5}$$

$$\frac{\partial P_i}{\partial \delta_k} = |V_i||V_k|[G_{ik} \sin(\delta_i - \delta_k) - B_{ik} \cos(\delta_i - \delta_k)] \tag{3.6}$$

ii.   **Sub-matrix $\dfrac{\partial Q}{\partial \delta}$:**

$$\frac{\partial Q_i}{\partial \delta_i} = \sum_{k=1, k \neq i}^{n} |V_i|\, |V_k|[G_{ik} \cos(\delta_i - \delta_k) + B_{ik} \sin(\delta_i - \delta_k)]$$

$$= P_i - G_{ii}V_i^2 \tag{3.7}$$

$$\frac{\partial Q_i}{\partial \delta_k} = -|V_i||V_k|[G_{ik} \cos(\delta_i - \delta_k) + B_{ik} \sin(\delta_i - \delta_k)] \tag{3.8}$$

iii.   **Sub-matrix $\dfrac{\partial P}{\partial |V|}$:**

$$V_i \frac{\partial P_i}{\partial |V_i|} = \sum_{k=1, k \neq i}^{n} |V_i|\, |V_k|[G_{ik} \cos(\delta_i - \delta_k) + B_{ik} \sin(\delta_i - \delta_k)] + 2G_{ii}|V_i|^2$$

$$= P_i + G_{ii}V_i^2 \tag{3.9}$$

$$V_k \frac{\partial P_i}{\partial |V_k|} = |V_i||V_k|[G_{ik} \cos(\delta_i - \delta_k) + B_{ik} \sin(\delta_i - \delta_k)] \tag{3.10}$$

iv. **Sub-matrix** $\dfrac{\partial \boldsymbol{Q}}{\partial |\boldsymbol{V}|}$:

$$V_i \frac{\partial Q_i}{\partial |V_i|} = \sum_{k=1,k\neq i}^{n} |V_i|\,|V_k|[G_{ik}\sin(\delta_i - \delta_k) - B_{ik}\cos(\delta_i - \delta_k)] - 2B_{ii}|V_i|^2 \tag{3.11}$$

$$= Q_i - B_{ii}V_i^2$$

$$V_k \frac{\partial Q_i}{\partial |V_k|} = |V_i||V_k|[G_{ik}\sin(\delta_i - \delta_k) - B_{ik}\cos(\delta_i - \delta_k)] \tag{3.12}$$

3.1.1.3 Ill- Conditioning

The load flow problem is said to be ill-conditioned if the Jacobian matrix is ill-conditioned. This is because in the Newton-Raphson algorithm, each iteration has the following linear form:

$$[J]\Delta \boldsymbol{x} = -\Delta \boldsymbol{S} \tag{3.13}$$

Where, $\Delta \boldsymbol{x} = \begin{bmatrix} \boldsymbol{\delta}_{k+1} \\ |\boldsymbol{V}|_{k+1} \end{bmatrix} - \begin{bmatrix} \boldsymbol{\delta}_{k} \\ |\boldsymbol{V}|_{k} \end{bmatrix}$ = bus voltage (magnitude and angle) correction vector

$\Delta \boldsymbol{S} = \begin{bmatrix} \Delta \boldsymbol{P}_k \\ \Delta \boldsymbol{Q}_k \end{bmatrix}$ = active and reactive power mismatch vector

Therefore, if the Jacobian matrix is ill-conditioned, the solution to the power flow iteration can become wildly unstable or divergent.

The most common characteristics that lead to ill-conditioned power flow problems are as follows.

- Heavily loaded power system (i.e. voltage stability problem where system has reached nose point/bifurcation point of real power vs. voltage- PV curve).
- Lines with high R/X ratios.
- Large system with many radial lines.
- Poor selection of the slack bus (e.g. in a weakly supported part of the network).

3.1.2 Load Flow Analysis using PSS®E

In this study, load flow analysis is performed in Power System Simulator for Engineering (PSS®E – often written as PSS/E). PSS®E is a software tool used by power system engineers to simulate electrical power transmission networks. This software is developed and supported by Siemens Power Technologies International (PTI) and it is used by various industries over

115 countries around the world for detailed planning and assessment of large-scale networks [46].

In this study, after building a test network in PSS®E, the load flow is performed by selecting Full Newton-Raphson method from the simulator.

3.2 Short-Circuit Ratio (SCR)

To define system strength of any wind dominated grid, an index is widely used named Short-Circuit Ratio (SCR).

3.2.1 Definition of SCR

If a wind power plant is connected to the grid, the SCR at the PCC is defined as the ratio between the short-circuit capacity at the PCC and the rated capacity of the wind power plant.

3.2.2 Method to Calculate SCR

To calculate SCR, IEC 60909 method is widely used [41]. This method is described below.

3.2.2.1 IEC 60909 Method

According to IEC 60909 method [47], the SCR at PCC i (i.e. bus i) can be calculated by equation (3.14).

$$SCR = \frac{S''^i_k}{P^i_{max}} \tag{3.14}$$

Where, P^i_{max} = Rated power of the wind power plant connected to bus i and

S''^i_k = Initial symmetrical short-circuit apparent power at bus i

The initial symmetrical short-circuit apparent power at bus i is the product of the initial symmetrical short-circuit current I''^i_k at bus i, the rated voltage V^i_n at bus i and $\sqrt{3}$ as shown in (3.15).

$$S''^i_k = \sqrt{3}I''^i_k V^i_n \tag{3.15}$$

In this method, Thevenin equivalent impedance is required. Thevenin equivalent short-circuit impedance Z^i_k is the impedance as seen from the i-th bus when a fault is applied at bus i. Then

the initial symmetrical short-circuit current, I''^i_k at bus i can be determined by (3.16). Also, c is a voltage factor which takes into consideration the voltage variations in the networks

$$I''^i_k = \frac{cV^i_n}{\sqrt{3}Z^i_k}$$

(3.16)

3.2.2.2 IEC Method via PSS®E

A balanced three phase fault is applied to the PCC and the initial symmetrical short-circuit current I''^i_k is calculated using IEC 60909 fault calculation tools of PSS®E software [46, 48]. The following steps are followed to perform short-circuit current calculation.

Step 1: A valid load flow working case is considered.

Step 2: Load flow solution is performed from the option Power Flow > Solution > Solve. Full Newton-Rapshon is selected as load flow solver and 'Flat Start' option used for initialization of load flow variables.

Step 3: The bus voltage V^i_n of the PCC bus is recorded after load flow. The voltage after load flow is used to be more precise.

Step 4: Before fault calculation, the PSS®E is set from the option Misc > Change Program Settings > Short Circuit. Under that window, the units of current, voltage and impedance are set to Physical and co-ordinates are set to Rectangular.

Step 5: The fault calculation is initialized from the menu using Fault > Setup for Special Fault Calculation. There, IEC909 fault calculation is selected, tap ratio is set to unity, charging capacitance is set to zero and switched shunts are set to zero in all sequences.

Step 6: Then the fault analysis is performed from Fault > IEC 60909 Fault Calculation Menu. Three phase fault is applied to simulate the most severe case. In addition, I"k contributions to "N" levels away is selected as output option. Also, the voltage factor C option for fault current calculation is set to 1.0. After that, in 'The Following Bus' option, the PCC buses are selected and run for simulation. Multiple fault calculation can be done by entering more than one buses.

The flowchart of calculating short-circuit current via PSS®E is given in Figure 3.1.

```
┌─────────────────────────────┐
│   Charging a valid load flow │
│        working case          │
└─────────────────────────────┘
              │
              ▼
┌─────────────────────────────┐
│     Performing load flow     │
│          solutions           │
└─────────────────────────────┘
              │
              ▼
┌─────────────────────────────┐
│  Recording bus voltage ($V_n^i$) │
└─────────────────────────────┘
              │
              ▼
┌─────────────────────────────┐
│  Setting appropriate settings│
└─────────────────────────────┘
              │
              ▼
┌─────────────────────────────┐
│         Initializing         │
└─────────────────────────────┘
              │
              ▼
┌─────────────────────────────┐
│   Performing fault analysis  │
└─────────────────────────────┘
```
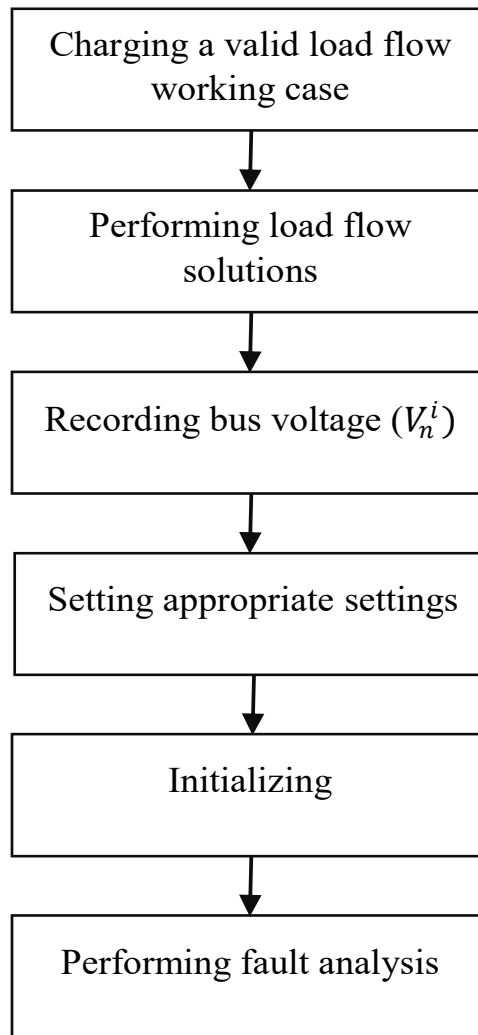
Figure 3.1: IEC 60909 method to determine fault current via PSS®E

The load flow gives V_n^i, IEC method gives I''^i_k and the P_{max}^i is known. Therefore, SCR can be calculated using (3.1) and (3.2).

3.3 Power System Network and Simulation Cases

3.3.1 System Modeling

The modified IEEE 39 bus test system is considered as a test network [49]. The total load of the system is 6356 MW. Investigations are performed in two stages- current situations (base case) and the foreseeable future situation (high wind power penetrated case). At the base case, there is no wind power plant in the power system. Then, four wind power plants are modelled installed consecutively to observe the SCR value at various wind penetration level. As such, SCR at four PCCs are studied at five different wind penetration scenarios. The simulation network is depicted in Figure 3.2. The wind plant PCCs are bus 14, 15, 16 and 20.

The system is constructed in PSS®E platform. All data related to bus, lines, generators, loads and transformers are given respectively in Table A.1, Table A.2, Table A.3, Table A.4 and Table A.5 in Appendix A.
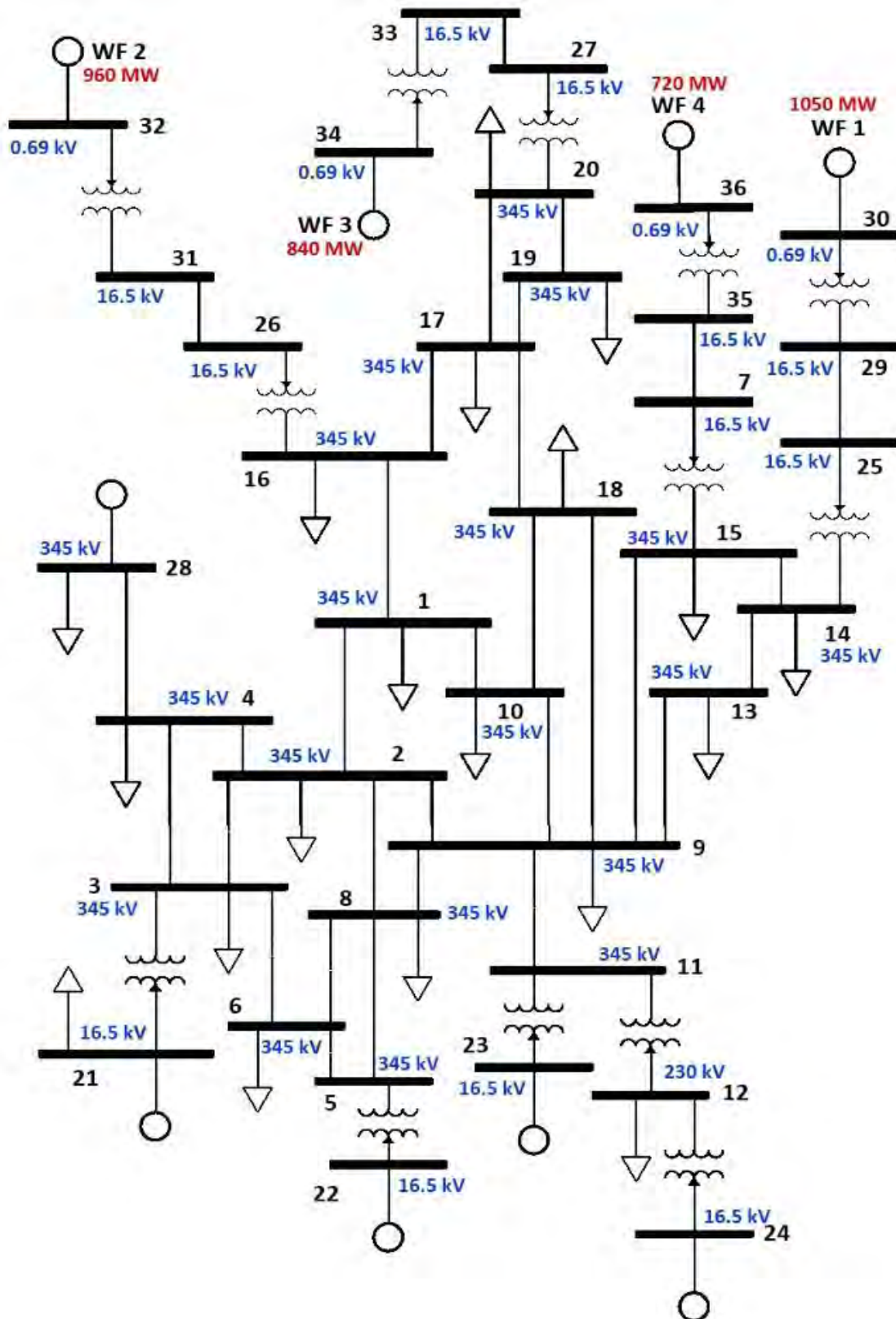
Figure 3.2: Test system with four wind power plants

3.3.2 Connection of Wind Power Plant

In this work, Type 3 WTGs are taken into account to model wind power plants [50] [51]. A typical connection diagram is shown in Figure 3.3. The common generation level for a WTG is 0.69 kV. Then a step up transformer of 0.69/16.5 kV is utilized. Afterwards, a transmission line is used to bring the wind generation into the grid. Finally, a 16.5/345 kV step up transformer is deployed to complete the connection.
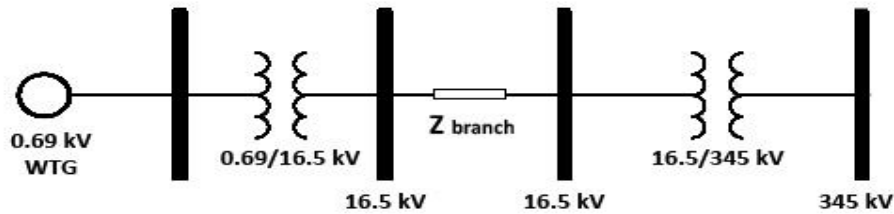
Figure 3.3: Typical connection diagram of a wind power plant

3.3.3 Simulation Cases

In this work, total five simulation cases with various wind penetration levels are considered. Note that wind penetration level is defined as the ratio between the total wind generation and total generation including wind and synchronous. The simulation scenarios are briefly described as follows.

- Case A: In this case, there is no wind farm in the system. All the generators are conventional synchronous generator. This case is considered to setup a baseline to understand the effect of wind penetration on the SCR.

- Case B: One wind power plant with the rated capacity of 1050 MW is added. It is linked to bus 14 in the power system network (refer to Figure 3.2). This wind plant supplies 840 MW to the grid. It creates 14% wind power penetration level.

- Case C: The second wind power plant with the rated capacity of 960 MW is connected. It is liked to bus 16. This wind plant supplies 768 MW to the grid. Two wind power plants produce 27% wind power penetration level.

- Case D: The third wind power plant with the rated capacity of 840 MW is added. This wind plant supplies 672 MW to the grid. The PCC for this wind plant is bus 20. The wind penetration level now increases to 38%.

- Case E: The fourth wind power plant with the rated capacity of 720 MW is installed. This wind plant supplies 576 MW to the grid. It is connected to bus 15 in the high voltage grid.

With all four wind power plants, the wind penetration level increases to 48%. Table 3.1 summarizes the simulation cases.

Table 3.1: Simulation cases

Case	No. of wind plants	Corresponding PCCs	Wind penetration Level
A	0	-	0%
B	1	14	14%
C	2	14, 16	27%
D	3	14, 16, 20	38%
E	4	14, 15, 16, 20	48%

3.4 Simulation Results and Analysis

A balanced three phase fault is applied to the PCCs using IEC 60909 fault calculation tools of PSS®E software. It is to be noted that for comparison with the high wind case, short-circuit analysis is performed in four PCCs at the base case by considering the scheduled capacities and locations of wind power plants [21]. The same concept is adopted for other cases. Simulation results are analyzed as follows.

3.4.1 Case A (Base Case)

In the base case i.e. Case A, there is no wind farm in the power system. Load flow analysis is done at the beginning to obtain pre-fault voltages at all buses. Then, three phase fault is sequentially applied at the selected PCCs. Fault current is recorded, which is used to calculate SCR values. Table 3.2 shows the SCR values at four PCCs in Case A. It can be seen that all SCR values are above 10. Therefore, when wind power penetration level is 0%, the system strength is significant. Also, bus 20 is the strongest bus in perspective of short-circuit performance.

Table 3.2: Value of SCR in Case A

Case A	
PCC bus	Value of SCR
14	10.35
16	11.16
20	11.18
15	10.63

3.4.2 Case B

In this case, wind penetration level increases to 14%. To facilitate the additional wind generation, some synchronous generators are replaced. As such, the amount of fault current reduces in the corresponding part of the network. Consequently, the SCR values drop as shown in Table 3.3. The most significant change is noticed at bus 14. In this bus, SCR decreases to 2.85 from 10.35 (compared to the base case). This is due to the fact that wind power plant is connected to this bus. Hence, the reduction in fault current becomes most prominent in this location. It eventually causes the SCR at bus 14 to drop below the minimum acceptable level (i.e. less than 3). In other buses, SCR also decreases. However, the reduction is less significant compared to bus 14. Also, bus 20 is still the strongest bus in terms of short-circuit enactment.

Table 3.3: Value of SCR in Case B

Case B	
PCC bus	Value of SCR
14	2.85
16	11.15
20	11.16
15	10.45

3.4.3 Case C

In this case, wind penetration increases to 27%. Two wind power plants are added in bus 14 and 16. Consequently, the value of fault current becomes less in theses buses. As a result, the SCR values decreases. In Table 3.4, the SCR at four PCCs are shown under 27%

wind penetration level. As observed from Table 3.4, the system strength is considerably affected in bus 16 (compared to case B) due to the placement of the new wind power plant in this location. In other buses, the SCR also shows decreasing trend.

Table 3.4: Value of SCR in Case C

Case C	
PCC bus	Value of SCR
14	2.74
16	3.12
20	10.94
15	10.44

3.4.4 Case D

In this case, a third wind power plant is integrated in bus 20. It results in 38% wind penetration level in the network. Table 3.5 outlines the SCR values in Case D. It can be noticed that in three PCCs (out of four), the SCR values drops below the minimum acceptable level. Also, bus 15 is the strongest bus regarding the short-circuit performance in this case.

Table 3.5: Value of SCR for Case D

Case D	
PCC bus	Value of SCR
14	2.68
16	2.90
20	2.65
15	10.41

3.4.5 Case E

In Case E, wind penetration level increases to 48% due to the presence of four wind power plants in the network. SCR values are calculated, which are shown in Table 3.6. It is seen that the SCR values are below the acceptable level (i.e. less than 3) in all four PCCs. It

indicates that the system strength significantly reduces when the wind penetration level increases in the network.

Table 3.6: Value of SCR in Case E

Case E	
PCC bus	Value of SCR
14	2.63
16	2.89
20	2.64
15	2.93

To clearly observe the trends of SCR in all PCCs with respect to wind penetration level, Figure 3.4 to 3.7 are plotted. These figures respectively show the SCR behavior in bus 14, 16, 20 and 15. It can be noticed in a specific bus, as wind penetration increases, the SCR exhibits decreasing trend. It further rationalizes the need of additional fault current contributing devices (e.g. synchronous condenser) under high wind power penetration.
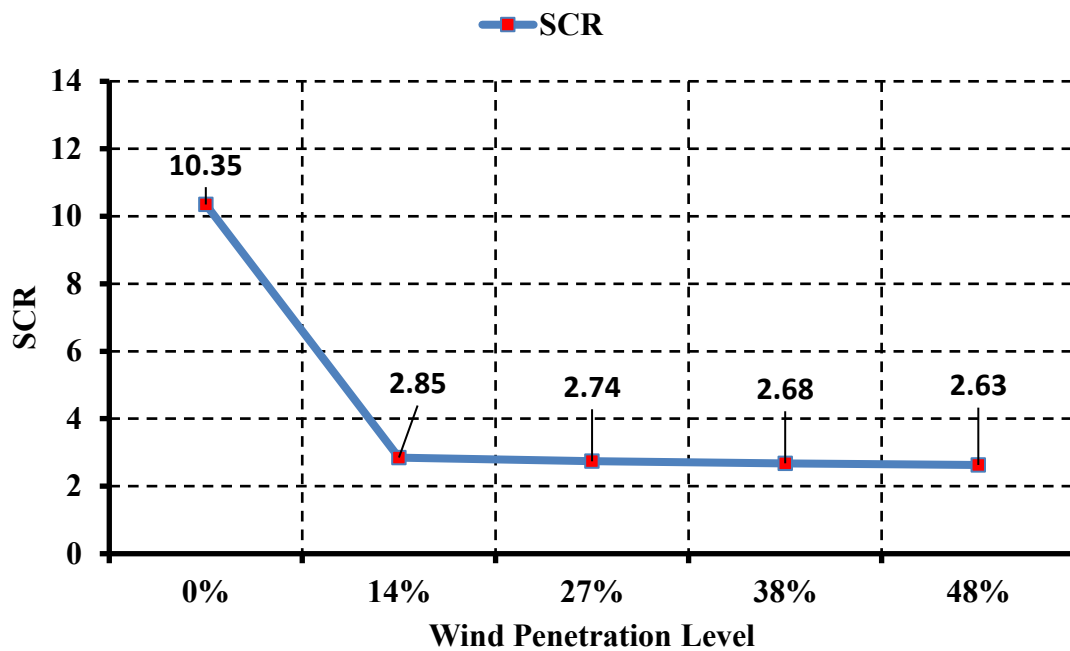
Figure 3.4: Trend of SCR values at bus 14

23
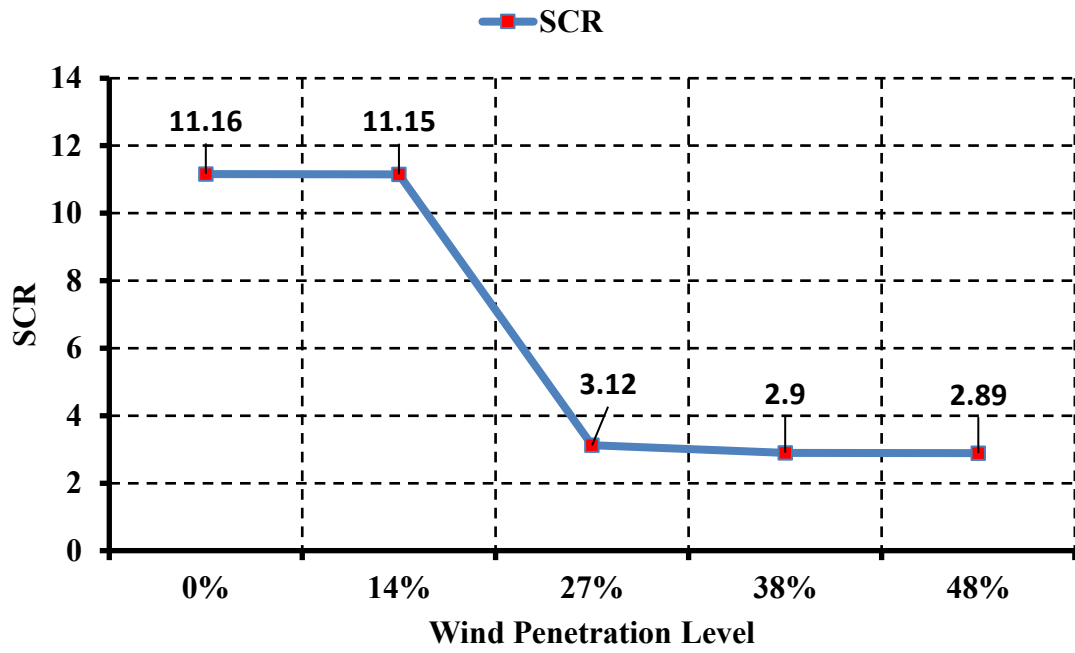
Figure 3.5: Trend of SCR values at bus 16
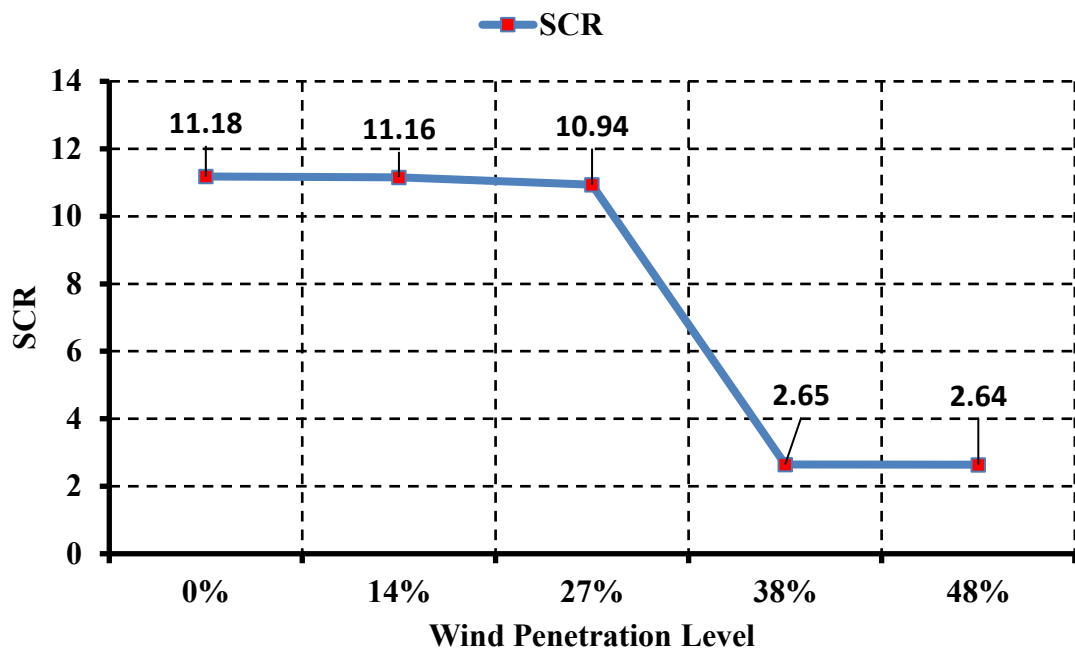
Figure 3.6: Trend of SCR values at bus 20
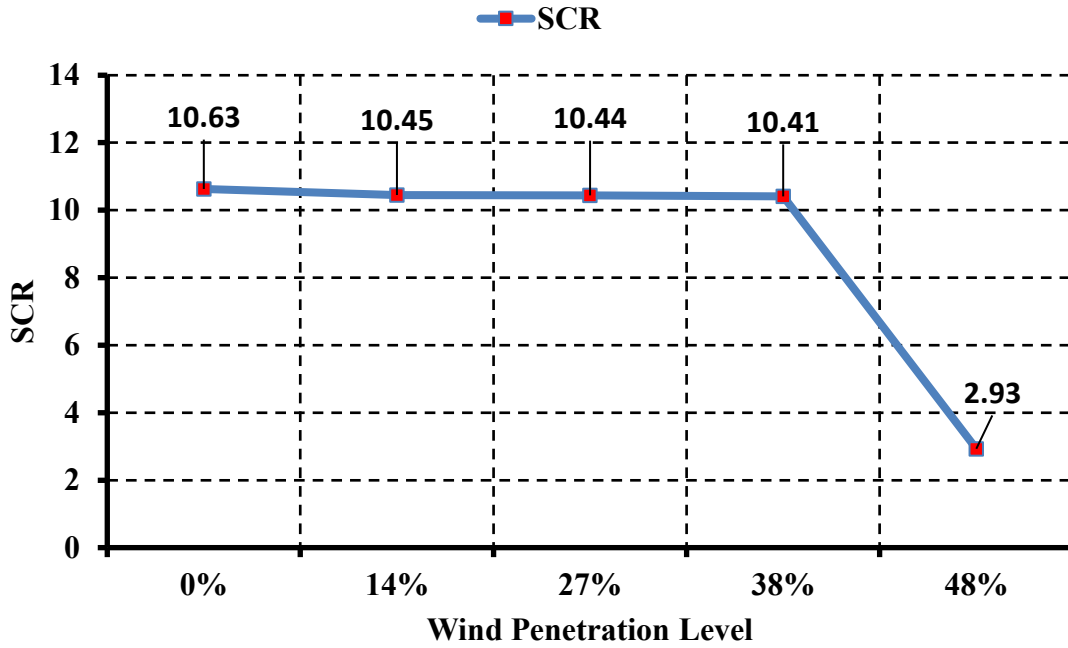
Figure 3.7: Trend of SCR values at bus 15

3.5 Synchronous Condenser

A synchronous condenser is basically a synchronous generator without any mechanical load. Synchronous condensers have been used for reactive power support before and are now employed through new installations or refurbishment of conventional generators or as standalone condensers for sustaining grid rotational inertia and short-circuit capacity [22, 41, 52]. A single-line diagram of synchronous condenser connected to the grid is depicted in Figure 3.8.

A synchronous condenser behaves akin to synchronous machine under fault. Therefore, it considerably contributes to fault current. Eventually, it assists to increase SCR, especially under high penetration of wind power.
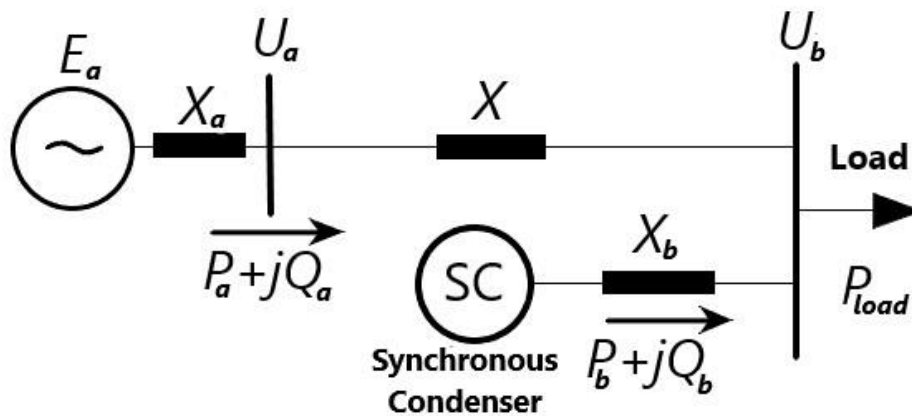
Figure 3.8: Schematic diagram of a synchronous condenser connected to the grid [53]

3.6 Effect of Synchronous Condenser on SCR

To demonstrate the effectiveness of synchronous condensers to enhance SCR, four synchronous condensers (SCs) are connected to the PCC of wind power plants. The highest wind penetration level (i.e. 48%) scenario is taken into account. The ratings are intuitively selected as 200 MVA, 100 MVA, 200 MVA and 100 MVA at bus 14, 15, 16 and 20 respectively.

Simulations are carried out after connecting the synchronous condensers. The values are outlined in Table 3.7. It can be noticed that SCR becomes higher than the minimum acceptable level in all four PCCs. Also, when the rating of synchronous condenser is larger, the improvement in SCR is more prominent.

Table 3.7: SCR value with and without SC at PCC Bus

PCC	Bus 14	Bus 15	Bus 16	Bus 20
SCR value without SC	2.68	2.93	2.89	2.64
SCR value with SC	4.35	3.10	3.76	3.37
Size of SC (MVA)	200	100	200	100

It should be noted that for this particular simulation, the size of synchronous condenser is instinctively selected. However, the sizes of the synchronous condensers need to be optimized because the installation of the synchronous condenser is expensive. Higher capacity of synchronous condenser would result in higher cost. The detailed optimization is presented in the next chapter.

3.7 Summery

It is found that system strength gradually decreases when wind penetration level increases. Also, synchronous condensers can be installed to improve system strength. It should be noted that in this chapter, the size of synchronous condenser is instinctively selected. However, the sizes of the synchronous condensers need to be optimized because the installation of the synchronous condenser is expensive. Higher capacity of synchronous condenser would result in higher cost. To address this issue, the detailed optimization technique to find the appropriate sizes of synchronous condensers is presented in the next chapter.

Chapter 4
Optimal Sizing of Synchronous Condensers

4.1 Introduction

In the previous chapter, it is clear that in a wind dominated system, the system strength is likely to reduce at the corresponding PCCs. To offset this situation, wind power plants are intentionally curtailed, which allows a certain number of synchronous generators online to provide sufficient system strength [54, 55, 56]. However, this eventually restricts the dispatch of wind power that leads to financial loss. As wind power plants usually have high capital cost ($/MW) but low operational costs ($/MWh), they should be operational as much as possible to pay back their capital costs. As a result, keeping additional conventional plants committed (despite having higher operational cost) is not a cost-effective solution while considering long-term techno-economic benefit. To overcome this challenge, deployment of synchronous condensers can be a promising solution.

As synchronous condensers are directly linked to the grid, they contribute to fault levels similar to synchronous generators. Since synchronous condensers are costly, to find their optimal sizes to maintain adequate system strength is a major query to investigate. Therefore, a methodology is proposed in this thesis to determine the optimum size of synchronous condensers while being the most economically viable. To this end, system strength is calculated based on IEC 60909 technique. Also, revenue and losses are modelled to investigate the long-term profit of deploying synchronous condensers. The optimization model is solved using Genetic Algorithm. The problem formulation, proposed approach and case studies are comprehensively presented as follows.

4.2 Problem Formulation

The optimization problem is described by an objective function and constraints. In this work, the objective function is to maximize the Net Present Value (NPV) of installing synchronous condensers in every PCC. In addition, the constraint to maintain SCR above the minimum value (i.e. 3) at every PCC of wind power plants. The problem formulation is stepwise described below.

4.2.1 Net Present Value (NPV)

NPV is the difference between the present value of cash inflows and the present value of cash outflows over a period of time [57]. Mathematically, NPV can be represented by (4.1).

$$NPV = \sum_{i=1}^{i=N_{years}} \frac{R_i - C_i}{(1+r)^i} - C_0 \qquad (4.1)$$

Where, N_{years} = number of years that the synchronous condensers will be in operation. The asset life of synchronous condenser is assumed to be 20 years in this work [58].

C_i	= the net costs during the i-th year
R_i	= the net revenues during the i-th year
C_0	= the installation cost of synchronous condensers
r	= the discount rate, which is set to 7% following [59].

4.2.2 Objective Function

The objective function and the constraint are given below as follows.

$$\max NPV(x) \qquad (4.2)$$
$$s.t \; SCR(x) \geq SCR_{min} \qquad (4.3)$$

Here,

x = the solution vector of size $N_{PCC}.1$ and N_{PCC} is the number of PCC under study. For this study, the number of synchronous condensers installed is 4 as there are 4 PCCs. The j-th row of x contains the information about the rating of the synchronous condenser installed at j-th PCC, which is optimized.

$SCR(x)$ = the vector containing the values of SCR of j-th PCC at its j-th row

SCR_{min} = the vector with the lowest acceptable limit of SCR that is considered as 3 in this study.

4.2.3 Cost Modelling

The cost of installing synchronous condensers C₀ is given by (4.4).

$$C_0(x) = \sum_{j=1}^{j=N_{PCC}} \{C_f + C_v S(x_j)\} g(x_j) \qquad (4.4)$$

Here, C_f = fixed cost ($) per synchronous condenser installed.

C_v = variable cost ($) per MVA installed

S = function that indicates the rating/size of synchronous condenser installed at a wind plant PCC

g = function that indicates the number of synchronous condenser installed at a wind plant PCC

Also, there is a maintenance cost per year C_{main} to operate synchronous condensers over a long period time. This cost can be formulated via (4.5).

$$C_{main}(x) = \sum_{j=1}^{j=N_{PCC}=4} C_{mavg}S(x_j) \qquad (4.5)$$

Where C_{mavg} = the averaged maintenance cost (\$/MVA per year).

In this study, C_f is set to 1 million US \$ [43], and C_v and C_{mavg} are assumed to be 30,000 US \$/MVA and 800 US \$/MVA per year [60].

Furthermore, because of the large ratings of the synchronous condensers and the continuous use of these devices, there are some electrical losses that come from the internal loss (P_{loss}) of synchronous condensers. This yearly cost (C_{elec}) is given by (4.6), where C_{MWH} is the yearly averaged cost of electricity (\$/MWh) [61] and τ_{SC} is the percentage of time the synchronous condensers are online. In this study, τ_{SC} is considered as 100% in order to see the viability of this study under the most conservative scenario.

$$C_{elec}(x) = 365 \times 24 \times \tau_{SC} C_{MWH} P_{loss} \times \sum_{j=1}^{j=N_{PCC}=4} S(x_j) \qquad (4.6)$$

The cost of electricity consumption of the synchronous condensers is directly linked to their internal losses (P_{loss}). As mentioned in [62], losses in synchronous condensers usually vary from 1.5% to 3% of their rated capacities. In this study, to consider a conservative scenario, P_{loss} is assumed to be 3%.

Therefore, the net cost is given by (4.7).

$$C_i = C_{main}^i + C_{elec}^i \qquad (4.7)$$

4.2.4 Revenue Modelling

Wind farms have experienced curtailment in some countries due to security concerns caused by high non-synchronous penetration [54, 55, 59, 63, 64]. Installing synchronous condensers would enhance SCR, which eventually will reduce wind curtailment.

Assume that synchronous condenser installation reduces wind curtailment by α%. The maximum wind curtailment reduction is assumed to be 6% [64]. In order to take into the conservative scenarios into account, 1% and 3% wind curtailment reductions are also analyzed.

The yearly revenue due to wind curtailment reduction (R_{wtg}) is obtained by installing synchronous condensers. Eventually, it is coming from the additional wind power sold, which is given by (4.8).

$$R_{wtg} = 365 \times 24 \times C_{MWH} \alpha P \qquad (4.8)$$

Where, P = averaged power output of wind farm

Besides, when wind power is curtailed, this shortfall is supplied by conventional fuel-based power plants. As such, extra fuel price needs to be paid. However, if wind power is not curtailed, this additional cost can be saved.

Yearly fuel saving (R_{fuel}) is given by (4.9).

$$R_{fuel} = 365 \times 24 \times C_{fuel} \alpha P \qquad (4.9)$$

Where, C_{fuel} = cost of fuel

All the data regarding average cost of electricity, cost of fuels, yearly averaged wind power production are collected based on [65].

Therefore, the net revenue is given by (4.10).

$$R_i = R_{wtg}^i + R_{fuel}^i \qquad (4.10)$$

4.3 Overview of the Studied Power System

The proposed methodology is applied to the test network described in section 3.3.1. The highest wind penetration case (i.e. 48% wind penetration level) is investigated. Four wind power plants are assumed to be installed in the network. Also, as found in section 3.4.5, there are four PCCs where the SCR values are lower than the minimum acceptable limit. The location rated capacity and SCR values at the PCCs of these wind power plants are shown in Table 4.1.

Table 4.1: Location, capacity, and SCR of wind power plants

PCC bus	Rated capacity (MW)	SCR
14	840	2.63
15	720	2.93
16	960	2.89
20	1050	2.64

The target of the optimization is to install synchronous condenser in each PCC in such a way that the sizes of the synchronous condensers are optimum, and it meets the objective function and constrain criteria mentioned in section 4.2.2.

4.4 Proposed Methodology

The optimization problem described in section 4.2 is non-linear because of SCR calculation. It is a multivariate constrained maximization problem. To solve this type of problem, Genetic Algorithm (GA) is widely used in various power system applications [66, 67, 68, 69].

4.4.1 Overview of Genetic Algorithm

GA is a search and optimization procedure that is motivated by the principles of natural genetics and natural selection. It was developed by J. Holland on the basis of Darwin's survival of the fittest theory in 1970 [70, 71]. Some fundamental ideas of genetics are borrowed and used artificially to construct search algorithm that is robust and require minimal problem information [72]. Genetic Algorithm is widely used because of its elegance and simplicity as well as its high performance to find the solutions for difficult high dimensional problems. [73, 74].

4.4.2 Implementation of the GA

The maximization problem of this study is, to maximize NPV, for synchronous condenser sizes that give an SCR value $\geqq$ SCR_{max} at every PCC bus. The statement follows that the fitness function is NPV(x) where x is the size of synchronous condensers at the desired fixed nodes or locations. The fitness function is multivariate. The number of locations is the number of unknown variables of the fitness function which is 4 in this study.

To implement a genetic algorithm, the necessary steps are as follows:

1. Starting with initial population
2. Doing crossover within that population
3. Doing mutation
4. Finding fit members
5. Calculating their fitness
6. Termination

Initialization: At the beginning, the process starts with a population/members or parents. For this study, these are the possible solutions i.e. sizes of condensers. For the initial population, let us assume there are n number of locations or nodes. Which means if the process starts with a P number of members (i.e.- size of population = P), each member of that population/parent chromosome S will have n number of genes. So, the population for ith generation,

$$g_i = (S_1, S_2, S_3, \ldots \ldots, S_P);$$

Where, $S_j = (X_{1j}, X_{2j}, X_{3j}, \ldots, X_{nj})$; $LB \leq X_{kj} \leq UB$; Given $i \in G, j \in P, k \in n$

In this study,

n = number of genes (locations) = 4

P = size of population = 25

G = maximum number of iteration/generations = 500

LB = lower bound (minimum size of synchronous condenser) = 1

UB = upper bound (minimum size of synchronous condenser) = 100

S = A member / parent chromosome (list of the size of synchronous condensers)

x = A gene (size of one synchronous condenser)

The iterators, i indicates generation and j indicates chromosome.

Crossover: For crossover, random uniform crossover is done in this study. The probability of crossover generally lies between 0.6 to 0.8 [75, 76]. The crossover rate is 50% in this study, since the number of genes is fairly small (n=4). To understand this, let us consider two parent chromosomes: S_1 and S_2. With a uniform crossover rate of 50% the Children $C_1^{(1,2)}$ and $C_2^{(1,2)}$ will look like this:

$$
\begin{array}{llllll}
S_1 & = & X_1^1, & X_2^1, & X_3^1, & X_4^1, \ldots\ldots\ldots, X_n^1 \\
S_2 & = & X_1^2, & X_2^2, & X_3^2, & X_4^2, \ldots\ldots\ldots, X_n^2 \\
C_1^{(1,2)} & = & X_1^1, & X_2^2, & X_3^1, & X_4^2, \ldots\ldots\ldots, X_n^2 \\
C_2^{(1,2)} & = & X_1^2, & X_2^1, & X_3^2, & X_4^1, \ldots\ldots\ldots, X_n^1 \\
\end{array}
$$

In short, every other gene of parent chromosome is swapped in the children chromosome. For a random uniform crossover, the places of this 50% of swapping are randomized. So t^{th} children chromosome $C_t^{(a,b)}$, crossover of parent chromosomes S_a and S_b will be:

$$C_t^{(a,b)} = X_{C1}^t, X_{C2}^t, X_{C3}^t, \dots\dots\dots, X_{Cn}^t$$

Where, $a \in P, b \in P, a \neq b \ t \in \ 2 \times^P C_2$ and $X_{Ck}^t = \left(X_k^a \ or \ X_k^b\right); k \in n$

Mutation: Mutation simply means changing genes within a chromosome to create new generation. If a mutation rate of m is chosen, for the tth child, $C_t^{(a,b)}$, after mutation the child will look like,

$$M_t = X_{m1}^t, X_{m2}^t, X_{m3}^t, \dots\dots\dots, X_{mn}^t$$

Where, $X_{mj}^t = X_{Cj}^t \pm \Delta x; \ \Delta x \in [0, m]; \ X_{mk}^t = X_{Ck}^t + \Delta x \leq UB; \ X_{mk}^t = X_{Ck}^t - \Delta x \geq LB$.

Probability of mutation generally lies between 0.001 to 0.1 [75, 76]. In this study, a 5% mutation rate is chosen for each cross over children.

Finding fit members: In this step, the constraint to find valid off-springs is checked. The children after crossover and mutation are checked to calculate,

$$SCR(M_t) = SCR(X_{m1}^t, X_{m2}^t, X_{m3}^t, \dots\dots\dots, X_{mn}^t)$$

and select only those children chromosomes, who satisfy the condition of having, the value of SCR $\geqq$ SCR_max. If no fit children chromosomes are found at any point of iteration/generation, the iteration is terminated.

Calculating fitness and selection: In this step, the fitness of the surviving off-springs is calculated. The survived/ constraint satisfying muted children chromosomes are used to calculate the fitness score (the calculation of NPV). A track of the best fit child and its fitness score are kept and pass the children for the next generation (i.e.- go back to step one), where these children are considered as parents.

Termination Condition: Either after the end of the iterations or when the termination condition is met where no fit children are found, the best fit solution/chromosome is found that maximizes the fitness function.

Figure 4.1 shows the steps of the Genetic Algorithm.
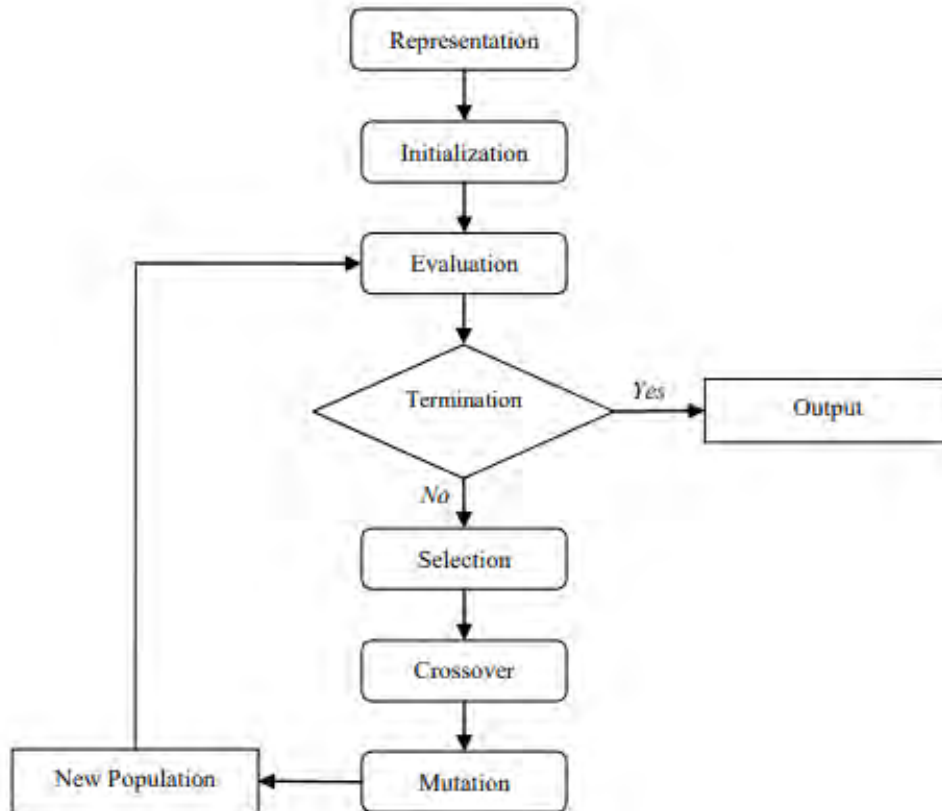
Figure 4.1: Steps of Genetic Algorithm [77]

4.5 Process Flow

In this study, the GA is developed in Python [78] and then it is incorporated with PSS®E. The following steps are maintained to implement the proposed algorithm.

- The test system is built in PSS®E and the optimization model is developed in Python. Effectively, a framework is developed consists of PSS®E and Python.

- Next, the GA randomly creates the initial population and sends it to PSS®E.

- Synchronous condensers are installed in every PCC in the network.

- Load flow analysis is performed via PSS®E and the voltages of all PCC buses are recorded. The load flow is executed using Python scripts.

- Then, short-circuit analysis is done in PSS®E using Python and SCR is calculated via IEC 60909 technique.

- PSS®E sends the results to GA, which creates the next generation, and this process goes on until the stopping criteria is fulfilled.

The whole process flow is illustrated in Figure 4.2.
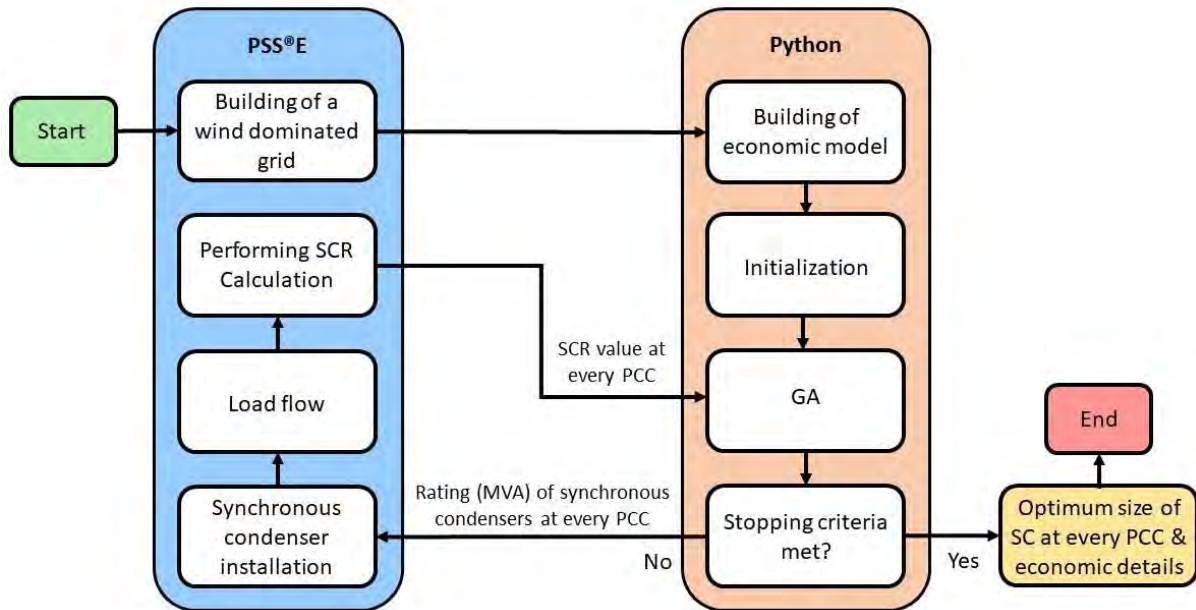
Figure 4.2: Flow graph of the implementation process.

4.6 Simulation Results and Analyses

4.6.1 Optimal Size of Synchronous Condenser

At first, SCR at the wind farm PCC are calculated without any synchronous condensers. For the optimization problem, synchronous condensers are installed in each of the four wind plants PCCs. The initial parent population is generated at random in a range of 1 to 100. The GA is run with a population size of 25 and maximum iteration of 500. The optimization model is solved and the optimal sizes of synchronous condensers (SCs) are obtained. Table 4.2 presents the results. Note that these values are valid for all wind curtailment reduction levels.

Table 4.2: Optimal sizes of synchronous condensers

PCC bus	Optimal size of SC (MVA)
14	81
15	5
16	20
20	68

Due to deployment of optimally sized synchronous condensers, the SCR values become satisfactory. Table 4.3 compares the SCR values at the wind power plants PCCs without and with synchronous condensers.

Table 4.3: Comparison of SCR

PCC bus	SCR without SC	SCR with SC
14	2.63	3.005
15	2.93	3.004
16	2.89	3.007
20	2.64	3.009

To analyze the influence of the synchronous condensers more precisely, fault current levels with and without synchronous condensers are compared in Figure 4.2. It can be seen that fault current increases by 1.75% to 12.5% due to the installation of the aforementioned synchronous condensers. Consequently, SCR also improves as shown in Table 4.3.
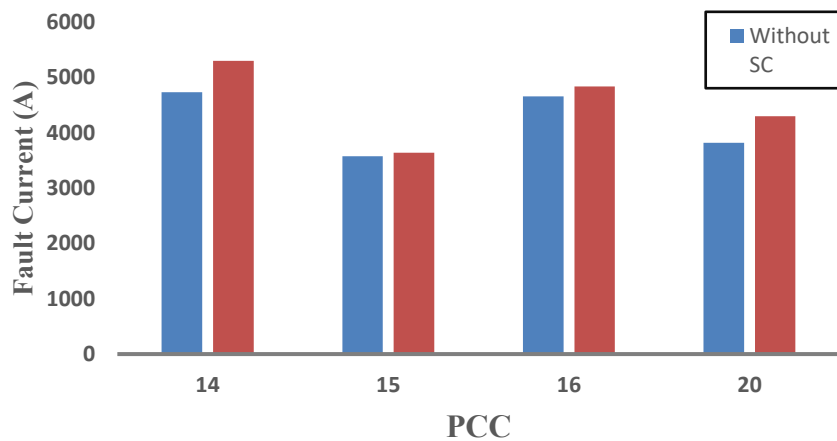
Figure 4.3: Fault current without and with synchronous condensers

4.6.2 Economic Analysis

4.6.2.1 NPV Calculation

To explore the long-term techno-economic benefit of optimally sized synchronous condensers, NPV is calculated. Note that wind curtailment reduction level affects the NPV values. As such three different wind curtailment reduction level such as 1%, 3% and 6% are taken into account. Moreover, the percentage of time for synchronous condensers being online is considered 100%, which is the most conservative approach. The NPV values after 20 years are given in Table 4.4.

Table 4.4: NPV values for different wind curtailment reduction

Wind curtailment reduction level (α)	NPV after 20 years (M US$)
1%	54.44
3%	557.47
6%	1312.00

It can be seen that the NPV values are positive even under the most conservative scenario. It implies that installation of synchronous condenser is economically viable. In fact, when synchronous condensers are installed, wind curtailment reduces. Thus, revenue is produced by trading additional wind power and saving of fossil fuel cost.

To explore the trend of NPV, Figure 4.4 is plotted. It shows the year-wise variation of NPV over 20 years' period for three wind curtailment reduction levels. It can be clearly seen that when wind curtailment reduction increases, the net economic benefit of installing synchronous condensers becomes more prominent.
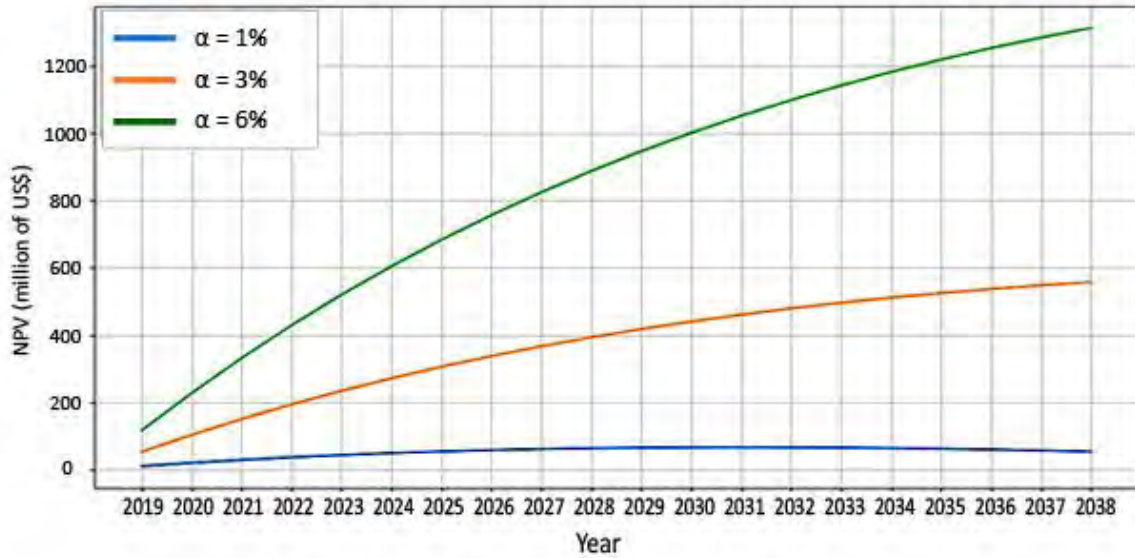
Figure 4.4: Trend of NPV for different wind curtailement reduction

4.6.2.2 Predominating Factor Affecting NPV

The revenue comes from additional wind power (due to reduction of wind curtailment level) and fuel savings. In order to find the predominating factor affecting economic benefits, the NPV is re-calculated considering the following cases one at a time.

    i.   with only fuel savings

    ii.   with only additionally sold wind power and

    iii.   with additionally sold wind power and fuel savings.

Figures 4.5, 4.6 and 4.7 depict the NPV curves for the above three scenarios under wind curtailment reduction level (α) of 1%, 3% and 6% respectively.

38
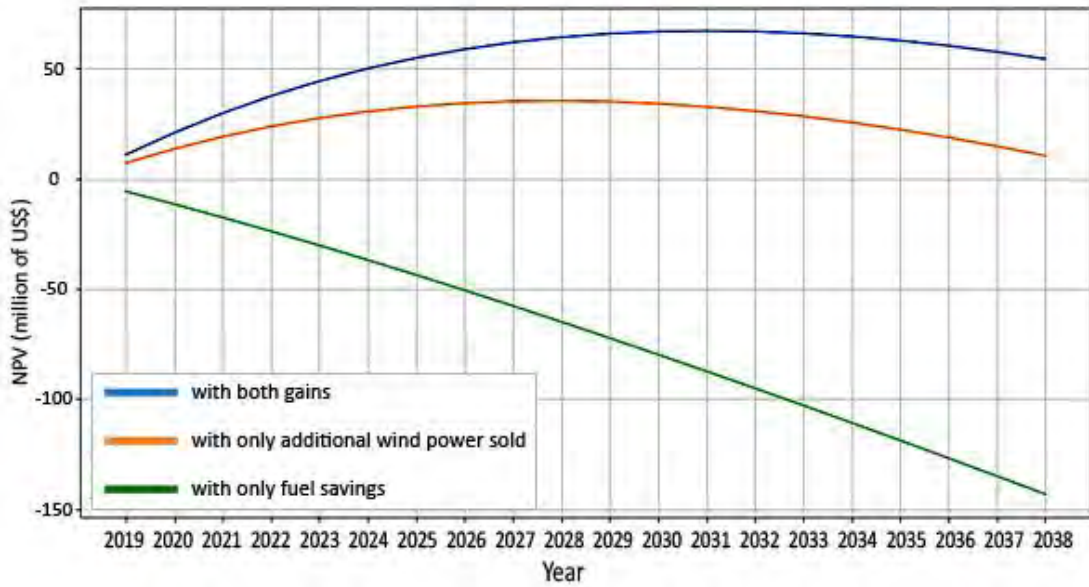
Figure 4.5: Influence of fuel savings and additionally sold wind power on NPV for α=1%.
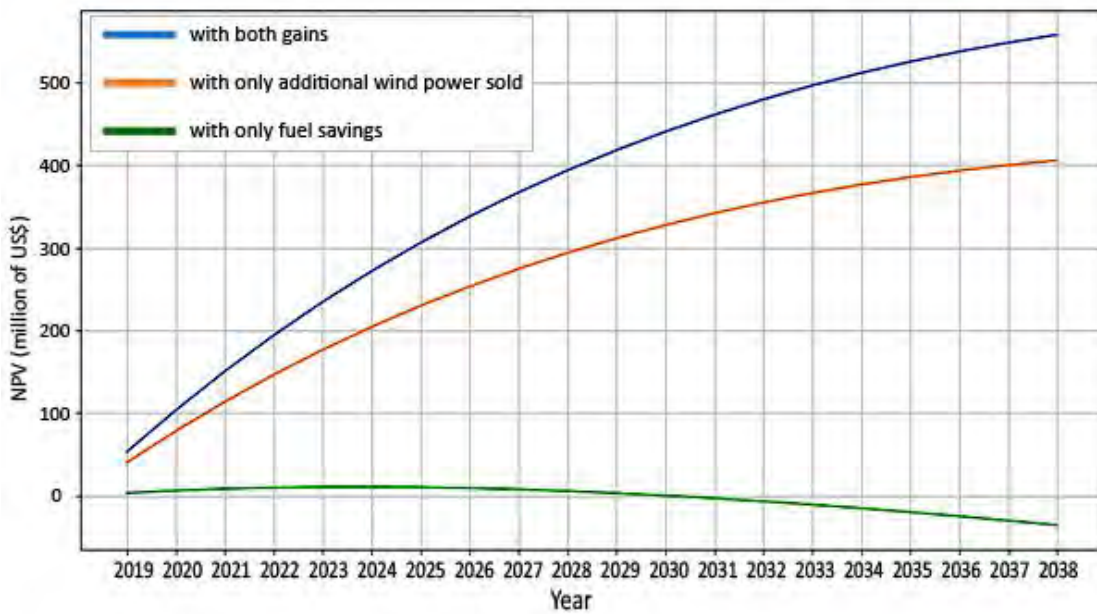
Figure 4.6: Influence of fuel savings and additionally sold power on NPV for α=3%
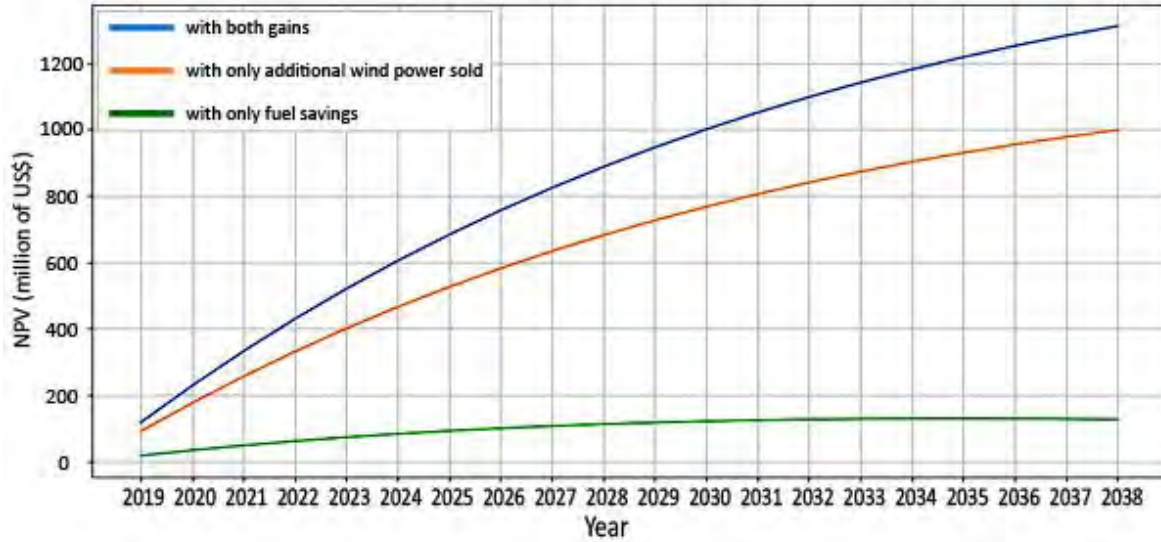
Figure 4.7: Influence of fuel savings and additionally sold power on NPV for α=6%

It is found that with only fuel savings, the NPV does not significantly change over time. Also, the NPV becomes negative (i.e. economically non-viable) for wind curtailment reduction factor of 1% and 3%. However, when only the additionally sold   qwind   power   is considered, the NPV shows increasing trend. The NPV becomes even larger when both case (i) and (ii) are considered together. Therefore, it can be concluded that the additionally sold wind power is the most prevailing factor for achieving economic benefits through optimal allocation of synchronous condensers.

4.6.2.3 Value Proposition of Synchronous Condensers

Installation of synchronous condensers increases the dispatch of wind generation. Therefore, producing power from wind plants instead of conventional synchronous generators causes fuel savings that ultimately brings economic benefits. These revenues (R^i) and also the costs (C^i) are comprehensively modelled in section 4.2.4 and 4.2.3 respectively. The value proposition of synchronous condensers is given by NPV, which is modelled in section 4.2.1.

Net profit of year i is calculated using as follows.

$$Net\ Profit^i = R^i - C^i \tag{4.12}$$

Tables 4.5 and 4.6 show the value proposition of synchronous condensers by showing NPV values and net profits in four years' interval for wind curtailment reduction (α) cases 3% and 6% respectively.

Table 4.5: Value proposition of synchronous condensers for α=3%

Year	4	8	12	16	20
Net Profit (M US$)	273.54	279.70	283.47	287.54	290.32
NPV (M US$)	194.30	337.82	440.36	511.33	557.47

Table 4.6: Value proposition of synchronous condensers for α=6%

Year	4	8	12	16	20
Net Profit (M US$)	551.36	563.72	571.27	579.48	585.07
NPV (M US$)	429.33	756.27	1000.63	1181.33	1312.00

The values shown in Tables are graphically represented in Figures 4.8 and 4.9 respectively. It is found that both NPV and net profit show increasing trends. This indicates that optimal sizing of synchronous condensers brings techno-economic benefits for network operators by reducing wind curtailment through the improvement of system strength. The more wind curtailment is avoided, the larger the benefits.
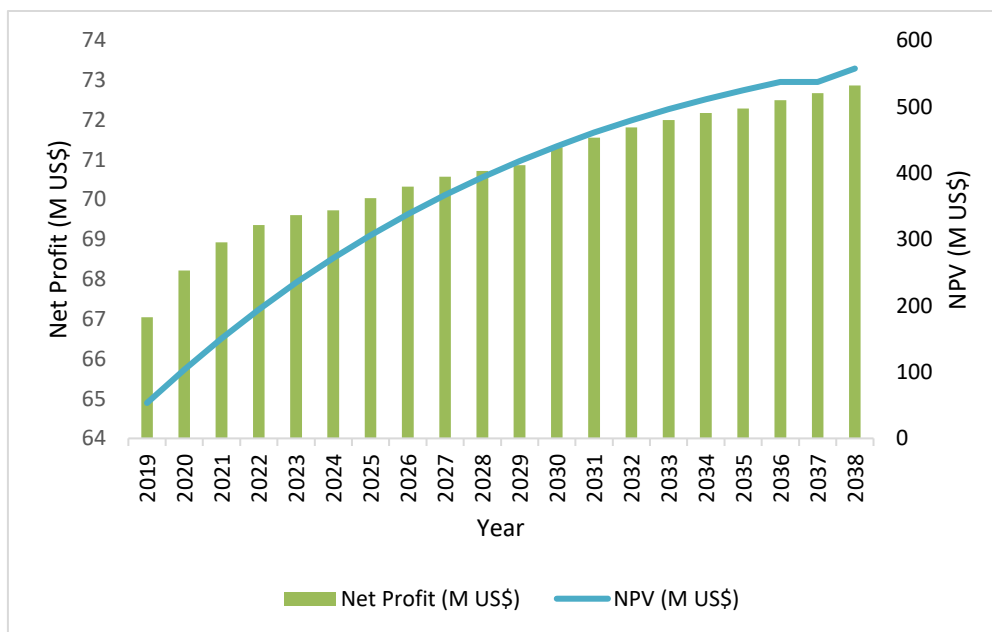
Figure 4.8: Net profit and NPV trend for α=3%
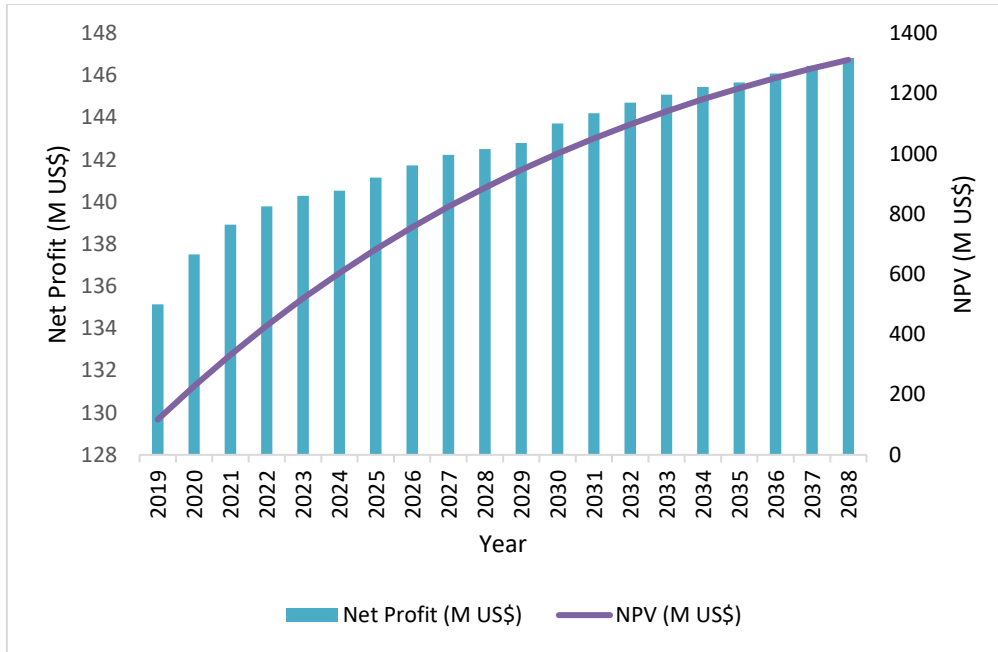
Figure 4.9: Net profit and NPV trend for α=6%

4.7 Validation of the Proposed Method

To validate the proposed methodology, its techno-economic benefit is compared with an existing technique. In the existing approach, sizes of synchronous condensers are intuitively chosen instead of finding them via optimization [22, 41]. To this end, four synchronous condensers instinctively selected and placed at four wind power plant PCCs. The ratings and SCR values are shown in Table 4.7.

Table 4.7: Ratings and SCR values for intuitively chosen synchronous condensers

PCC	Bus 14	Bus 15	Bus 16	Bus 20
Size of SC (MVA)	200	100	200	100
SCR value with SC	4.35	3.10	3.76	3.37

It is clear that with this above selection, SCR values considerably increase. However, to fully comprehend the benefit of optimally sized synchronous condensers, NPV values need to be compared. As such, NPV values are evaluated for intuitively selected synchronous condensers for three different wind curtailment reduction levels over 20 years' period. The values are then compared with that of optimally sized synchronous condensers, which are shown in Table 4.8.

42

Table 4.8: Comparison of NPV for validation

Wind curtailment reduction level	NPV for optimally sized synchronous condensers (M US$)	NPV for intuitively sized synchronous condensers (M US$)
1%	54.44	20.35
3%	557.47	275.45
6%	1312.00	1029.98

It can be clearly seen that optimally sized synchronous condensers provide more long-term economic benefit than the intuitively sized synchronous condensers. This is because for random sizing, the installation, operation and maintenance costs of synchronous condensers are relatively higher. Consequently, it offers less financial benefit compared to the proposed method. Therefore, it can be revealed that the optimal sizing technique presented in this work outperforms the existing approach. It also brings long-term techno-economic advantages for system operators, especially in a wind dominated power grid.

Chapter 5

Conclusions and Recommendation for Future Research

5.1 Conclusion

Short-circuit performance are considered as one of the foremost challenges in the perspective of power system security due to increased wind generation. Extensive analyses are carried out in this thesis to investigate the implications of high wind penetration on system strength. A methodology is proposed to facilitate the proliferated wind generation while maintaining adequate system strength. The key finds of this research work are summarized as follows.

i. As the wind penetration increases, the SCR at the PCC of wind power plants decreases.

ii. Being a rotating machine, a synchronous condenser contributes to fault current. Therefore, it helps to improve the system strength.

iii. The GA provides the optimum size of synchronous condenser to maintain the minimum values of SCR at the PCC of wind power plants. The SCR values are found to be satisfactory for all PCC buses under high wind power penetration.

iv. Operation time for synchronous condensers is assumed to be 100% while calculating NPV to consider the most conservative perspective. The NPV is positive over the 20 years' period after installing optimally sized synchronous condensers. It indicates the techno-economic benefits of the proposed algorithm.

v. The value of NPV for optimally sized synchronous condenser is higher than that of intuitively sized synchronous condenser installation. It implies that the optimally sized synchronous condenser provides more financial benefit than the intuitive sizing approach.

vi. It is observed that wind curtailment can be reduced by installing synchronous condensers to enhance system strength. Thus, it brings advantages for system operators as well as for wind plant owners.

vii. The revenue mostly comes from the selling of additional wind power (i.e. due to wind curtailment reduction). However, NPV increases when fuel cost saving is considered along with additionally sold wind power. Nonetheless, saving of fuel cost alone does not offer sufficient profits.

viii.   The net profit and NPV both show increasing trends positive rise over the 20 years' period. It indicates the possibility of large-scale integration of wind power while taking into account the technical and financial viabilities.

5.2 Recommendations for Future Works

The following scopes can be recommended for future researchers and engineers.

i.   Deployment of other devices that contribute fault currents, such as SVC (Static VAR Compensator) and STATCOM, for improving system strength can be explored.

ii.   Along with system strength, frequency response is another critical security parameter for wind dominated grids. Therefore, a platform can be developed to simultaneously improve system strength and frequency response in a wind prolific power system.

iii.   An algorithm can be derived to formulate optimal generation dispatch policy by taking into account system strength.

iv.   Maximum wind penetration level can be determined to maintain satisfactory system strength in a power system.

References

[1] "Global Wind Report 2019," Global Wind Energy Council (GWEC), 2019. [Online]. Available: https://gwec.net/global-wind-report-2019/. [Accessed March 2020].

[2] "Future of Wind-Deployment, investment, technology, grid integration and socio-economic aspects," International Renewable Energy Agency (IRENA), 2019. [Online]. Available: https://www.irena.org/media/Files/IRENA/Agency/Publication/2019/Oct/IRENA_Future_of_wind_2019.pdf. [Accessed March 2020].

[3] J. Ekanayak and N. Jenkins, "Comparison of the response of doubly fed and fixed-speed induction generator wind turbines to changes in network frequency," *IEEE Transactions on Energy conversion,* vol. 19, no. 4, pp. 800-802, 2004.

[4] J. Fletcher and J. Yang, "Introduction to the doubly-fed induction generator for wind power applications," INTECH Open Access Publisher, 2010. [Online]. Available: http://cdn.intechopen.com/pdfs/12519.pdf. [Accessed July 2019].

[5] M. Singh and S. Santoso, "Dynamic models for wind turbines and wind power plants," National Renewable Energy Laboratory, 2011. [Online]. Available: https://www.nrel.gov/docs/fy12osti/52780.pdf. [Accessed July 2019].

[6] F. O. Igbinovia, G. Fandi, I. Ahmad, Z. Muller and J. Tlusty, "Modeling and Simulation of the Anticipated Effects of the Synchronous Condenser on an Electric-Power Network with Participating Wind Plants," *Sustainability, MDPI, Open Access Journal,* vol. 10, no. 12, pp. 1-17, 2018.

[7] W. Jin and Y. Lu, "Stability Analysis and Oscillation Mechanism of the DFIG-Based Wind Power System," *IEEE Access,* vol. 7, p. 88 937–88 948, 2019.

[8] J. Xia, A. Dy. ko and J. O'Reilly, "Future Stability Challenges for the UK Network with High Wind Penetration Levels," *IET Generation, Transmission & Distribution,* vol. 9, no. 3, pp. 1160-116, 2015.

[9] World Wind Energy Association (WWEA), 2020. [Online]. Available: https://wwindea.org/blog/2020/04/16/world-wind-capacity-at-650-gw/. [Accessed April 2020].

[10] "Global Wind Installations," Wind Energy International, 2020. [Online]. Available: https://library.wwindea.org/global-statistics/. [Accessed March 2020].

[11] "National Database of Renewable Energy," [Online]. Available: http://www.renewableenergy.gov.bd/. [Accessed August 2020].

[12] G. Shafiullah, A. M. Oo, A. S. Ali and P. Wolfs, "Potential challenges of integrating large-scale wind energy into the power grid–A review," *Renewable and Sustainable Energy Reviews,* vol. 20, pp. 306-321, 2013.

[13] T. Ayodele, A. Jimoh, J. Munda and J. Agee, "Challenges of Grid Integration of Wind Power on Power System Grid Integrity: A Review," *International Journal of Renewable Energy Research,* vol. 2, no. 4, 2012.

[14] P. S. Georgilakis, "Technical Challenges Associated with The Integration of Wind Power into Power Systems," *Renewable and Sustainable Energy Reviews,* vol. 12, pp. 852-863, 2008.

[15] D. Weisser and R. S. Garcia, "Instantaneous Wind Penetration in Isolated Electricity Grids:Concepts and Review," *Renewable Energy,* vol. 30, pp. 1299-1308, 2005.

[16] L. Shang, J. Hu, X. Yuan and Y. Chi, "Understanding Inertial Response of Variable-Speed Wind Turbines by Defined Internal Potential Vector," *Energies,* vol. 10, no. 22, 2017.

[17] G. Lalor, A. Mullane and M. O'Malley, "Frequency control and wind turbine technologies," *IEEE Transactions on Power Systems,* vol. 20, no. 4, pp. 1905-1913, 2005.

[18] J. F. Conroy and R. Watson, "Frequency response capability of full converter wind turbine generators in comparison to conventional generation," *IEEE Transactions on Power Systems,* vol. 23, no. 2, pp. 649-656, 2008.

[19] B. Hartmann, I. Vokony and I. Táczi, "Effects of decreasing synchronous inertia on power system dynamics—Overview of recent experiences and marketisation of services," *International Transaction on Electrical Energy System,* vol. 29, no. 12, 2019.

[20] H. Ye, W. Pei and Z. Qi, "Analytical Modeling of Inertial and Droop Responses From a Wind Farm for Short-Term Frequency Regulation in Power Systems," *IEEE Transactions on Power Systems,* vol. 31, no. 5, pp. 3414-3423, 2016.

[21] S. Ghosh, S. Kamalasadan, N. Senroy and J. Enslin, "Doubly Fed Induction Generator (DFIG)-Based Wind Farm Control Framework for Primary Frequency and Inertial

Response Application," *IEEE Transactions on Power Systems,* vol. 31, no. 3, pp. 1861-1871, 2016.

[22] N. Masood, R. Yan, T. Saha and S. Barlett, "Post-Retirement Utilisation of Synchronous Generators to Enhance Security Performances in a Wind Dominated Power System," *IET Generation, Transmission & Distribution,* vol. 10, no. 13, pp. 3314-3321, 2016.

[23] A. Yogarathinam, J. Kaur and N. Chaudhuri, "Impact of Inertia and Effective Short Circuit Ratio on Control of Frequency in Weak Grids Interfacing LCC-HVDC and DFIG-Based Wind Farms," *IEEE Transactions on Power Delivery,* vol. 32, no. 4, pp. 2040-2051, 2017.

[24] R. Walling, E. Gursoy and B. English, "Current contributions from type 3 and type 4 wind turbine generators during faults," pp. 1-6, 2011.

[25] J. Morren and S. W. d. Haan, "Short-circuit current of wind turbines with doubly fed induction generator," *IEEE Transactions on Energy conversion,* vol. 22, no. 1, pp. 174-180, 2007.

[26] V. Gevorgian and E. Muljadi, "Wind power plant short-circuit current contribution for different fault and wind turbine topologies," 9th International Workshop on Large Scale of Wind Power into Power Systems, Quebec City, Quebec, Canada, 2010.

[27] "IEEE Guide for Planning DC Links Terminating at AC Locations Having Low Short-Circuit Capacities," in *IEEE Std 1204-1997*, IEEE, 1997.

[28] J. W. Feltes and B. S. Fernandes, "Wind turbine generator dynamic performance with weak transmission grids," IEEE Power and Energy Society General Meeting, San Diego, California, USA, 2012.

[29] S. D. Ahmed, F. S. M. Al-Ismail, M. Shafiullah, F. A. Al-Sulaiman and I. M. El-Amin, "Grid Integration Challenges of Wind Energy: A Review," *IEEE Access,* vol. 8, pp. 10857-10878, 2020.

[30] D. Devaraj and R. Jeevajyothi, "Impact of wind turbine systems on power system voltage stability," in *International Conference on Computer, Communication and Electrical Technology (ICCET)*, Tamilnadu, 2011.

[31] M. H. Albadi and E. F. El-Saadany, "Overview of wind power intermittency impacts on power systems," *Electric Power Systems Research,* vol. 80, no. 6, p. 627–632, 2010.

[32] T. Thiringer, T. Petru and S. Lundberg, "Flicker contribution from wind turbine installations," *IEEE Transactions on Energy Conversion,* vol. 19, no. 1, pp. 157-163, 2004.

[33] K. Yang, "Harmonic aspects of wind power integration," *Journal of Modern Power System and Clean Energy,* vol. 1, no. 1, pp. 14-21, 2013.

[34] U. Vargas and A. Ramirez, "Extended Harmonic Domain Model of a Wind Turbine Generator for Harmonic Transient Analysis," *IEEE Transactions on Power Delivery,* vol. 31, no. 3, p. 1360–1368, 2016.

[35] A. Reis, L. P. Moura and J. C. d. Oliveira, "Mitigation of harmonic current produced by wind turbine throughout converter switching control," in *17th International Conference on Harmonics and Quality of Power*, 2016 .

[36] C. Pazhanimuthu and S. Ramesh, "Grid integration of renewable energy sources (RES) for power quality improvement using adaptive fuzzy logic controller based series hybrid active power filter," *Journal of Intelligent {&} Fuzzy Systems,* vol. 35, no. 1, p. 749–766, 2018.

[37] G. Giebel and G. Kariniotakis, "Wind power forecasting—a review of the state of the art," Renewable Energy Forecasting, Elsevier, 2017.

[38] Q. Wang, C. B. Martinez-Anido, H. Wu, A. R. Florita and B. M. Hodge, "Quantifying the Economic and Grid Reliability Impacts of Improved Wind Power Forecasting," *IEEE Transactions on Sustainable Energy,* vol. 7, no. 4, pp. 1525-1537, 2016.

[39] J. J. Grainger and W. D. Steven, Power System Analysis, 1994.

[40] H. Gu, R. Yan and T. Saha, "Review of System Strength and Inertia Requirements for the National Electricity Market of Australia," *CSEE Journal of Power and Energy Systems,* vol. 5, no. 3, pp. 295-305, 2019.

[41] E. Marrazi, Y. Guangya and P. Weinreich-Jensen, "Allocation of Synchronous Condensers for Restoration of System Short-Circuit Power," *Journal of Modern Power Systems and Clean Energy,* vol. 6, no. 1, pp. 17-26, 2018.

[42] Y. Zhang, S. Huang, J. Schmall and et al, "Evaluating system strength for large-scale wind plant integration," *IEEE Power and Energy Society General Meeting, MD, U.S.,* pp. 1-5, 2014.

[43] J. Jia, G. Yang, A. Nielsen, P. Weinreich-Jensen, E. Muljadi and V. Gevorgian, "Synchronous Condenser Allocation for Improving System Short Circuit Ratio," in *IEEE 5th International Conference on Electric Power and Energy Conversion Systems*, 2018.

[44] D. Wu, G. Li, M. Javadi, M. Malyscheff, M. Hong and J. Jiang, "Assessing Impact of Renewable Energy Integration on System Strength Using Site-Dependent Short Circuit Ratio," *IEEE Transactions on Sustainable Energy,* vol. 9, no. 3, pp. 1072-1080, 2018.

[45] "Newton-Raphson Power Flow," [Online]. Available: https://wiki.openelectrical.org/index.php?title=Newton-Raphson_Power_Flow.

[46] "Power system simulator for engineering. PSS®E," [Online]. Available: https://new.siemens.com/global/en/products.html. [Accessed June 2019].

[47] "IEC 60909 short-circuits currents in three-phase AC systems," International Electrotechnical Commission (IEC), 2001.

[48] "PSS/E User Manual, Version 32," Program Application Guide: vol. I and II, PSS®E.

[49] M. A. Pai, Energy Function Analysis for Power System Stability, Boston, Dordrecht, London: Kluwer, Academic Publishers, 1st edition, 1989.

[50] "User Manual, PSS®E Wind Modeling Package for GE 1.5/1.6/2.5/2.75/4.0 MW Wind Turbine," Siemens, August, 2011.

[51] K. Clark, N. W. Miller and J. J. Sanchez-Gasca, "Modelling of GE wind turbine-generators for grid studies," GE Energy, 2010.

[52] A. Glaninger-Katschnig, "Contribution of synchronouscondensers for the energy transition. Electronics and Electrical Engineering," *Elektrotechnik und Informationstechnik,* vol. 130, no. 1, pp. 28-32, 2013.

[53] S. Teleke, T. Abdulahovic, T. Thiringer and J. Svensson, "Dynamic Performance Comparison of Synchronous Condenser and SVC," *IEEE Transactions on Power Delivery,* vol. 23, no. 3, pp. 1606-1612, 2008.

[54] M. M. Almenta, D. J. Morrow, R. J. Best, B. Fox and A. M. Foley, "An analysis of wind curtailment and constraint at a nodal level," *IEEE Transactions on Sustainable Energy,* vol. 8, no. 2, p. 488–495, 2017.

[55] X. Chen, M. B. McElroy and C. Kang, "Integrated energy systems for higher wind penetration in China: Formulation, implementation, and impacts," *IEEE Trans. Power Syst.,* vol. 33, no. 2, p. 1309–1319, 2018.

[56] J. Li, Y. Fu, Z. Xing, X. Zhang, Z. Zhang and X. Fan, "Coordination scheduling model of multi-type flexible load for increasing wind power utilization," *IEEE Access,* vol. 7, p. 105840–105850, 2019.

[57] G. Heydt, "The Probabilistic Evaluation of Net Present Value of Electric Power Distribution Systems Based on the Kaldor–Hicks Compensation Principle," *IEEE Transactions on Power Systems,* vol. 33, no. 4, pp. 4488-4495, 2018.

[58] ElectraNet, "Synchronous Condenser Asset Life Review," 2017. [Online]. Available: https://www.aer.gov.au .

[59] "National Transmission Network Development Plan," Australian Energy Market Operator (AMEO), Melbourne, VIC, Australia, 2018.

[60] F. Li, J. D. Kueck, D. T. Rizy and T. King, "A preliminary analysis of the economics of using distributed energy as a source of reactive power supply," Oak Ridge Nat. Lab, ORNL/TM-2006/014, Oak Ridge, TN, USA, Tech. Rep, 2006.

[61] Australian Energy Market Operator (AEMO), [Online]. Available: https://aemo.com.au/en/energy-systems/electricity/national-electricity-market-nem/data-nem/data-dashboard-nem. [Accessed January 2020].

[62] M. Nambiar and Z. Konstantinovic, "Impact of using synchronous condensers for power system stability and improvement of short-circuit power in mining projects," *Mining Eng,* vol. 67, pp. 38-44, 2015.

[63] E. V. M. Garrigle, J. P. Deane and P. G. Leahy, "How much wind energy will be curtailed on the 2020 irish power system?," *Renew. Energy,* vol. 55, pp. 544-553, 2013.

[64] "How much wind-powered electricity production has been curtailed in South Australia?," WattClarity, Global Roam, 2017. [Online]. Available: http://www.wattclarity.com.au/2017/09/.

[65] NTNDP database, AEMO, 2018. [Online]. Available: https://aemo.com.au/energy-systems/major-publications/integrated-system-plan-isp/national-transmission-network-development-plan-ntndp/ntndp-database. [Accessed November 2019].

[66] K. Nara, "Genetic algorithm for power systems planning," *Int. Conf. Adv. Power Syst. Control, Operation Manage. (APSCOM),* vol. 1, pp. 60-65, 1997.

[67] S. N. Singh and S. C. Srivastava, "Genetic Algorithm and its Applications to Power System problems," in *Proc. of 10th National Power System Conference*, Vadodara, 1998.

[68] Y. Gao and R. Billinton, "Adequacy assessment of generating systems containing wind power considering wind speed correlation," *IET Renewable Power Generation,* vol. 3, no. 2, pp. 217 - 226, 2009.

[69] F. B. Alhasawi and J. V. Milanovic, "Techno-Economic Contribution of FACTS Devices to the Operation of Power Systems with High Level of Wind Power Integration," *IEEE Transactions on Power Systems,* vol. 27, no. 3, pp. 1414 - 1421, 2012.

[70] L. Haldurai, T. Madhubala and R. Rajalakshmi, "A Study on Genetic Algorithm and its Applications," *International Journal of Computer Sciences and Engineering,* vol. 4, no. 10, pp. 139-143, 2016.

[71] M. Tabassum and K. Mathew, "A Genetic Algorithm Analysis towards Optimization solutions," *International Journal of Digital Information and Wireless Communications (IJDIWC),* vol. 4, no. 1, pp. 124-142, 2014.

[72] K. Deb, "An introduction to genetic algorithms," *Sadhana,* vol. 24, p. 293–315, 1999.

[73] "Genetic Algorithm," Science Direct, [Online]. Available: https://www.sciencedirect.com/topics/engineering/genetic-algorithm.

[74] A. Meyer-Baese and VolkerSchmid, "Chapter 5 - Genetic Algorithms," in *Pattern Recognition and Signal Analysis in Medical Imaging (Second Edition)*, Academic Press, 2014, pp. 135-149.

[75] N. N. Schraudolph and R. K. Belew, "Dynamic Parameter Encoding fo Genetic Algorithms," *Machine Learning,* vol. 9, pp. 9-21, 1992.

[76] J. J. Grefenstette, "Optimization of Control Parameters for Genetic Algorithm," *IEEE Trans. on Systems, Man and Cybernetics,* vol. 16, pp. 122-128, 1986.

[77] R. Entezari-Maleki and A. Movaghar, "A Genetic Algorithm to Increase the Throughput of the Computational Grids," *International Journal of Grid and Distributed Computing,* vol. 4, no. 2, 2011.

[78] Python 2.7, [Online]. Available: https://www.python.org/.

Appendix A: Test System Data

Table A.1 Data of voltage level of buses

Bus No.	Voltage (kV)
1	345
2	345
3	345
4	345
5	345
6	345
7	16.5
8	345
9	345
10	345
11	345
12	230
13	345
14	345
15	345
16	345
17	345
18	345
19	345
20	345
21	16.5
22	16.5
23	16.5
24	16.5
25	16.5
26	16.5
27	16.5
28	345

29	16.5
30	0.7
31	16.5
32	0.7
33	16.5
34	0.7
35	16.5
36	0.7

Table A.2 Line data

Line No.	From Bus	To Bus	R (p.u.)	X (p.u.)
1	1	2	0.0013	0.0213
2	1	10	0.0011	0.0133
3	1	16	0.0513	0.0600
4	2	3	0.0010	0.1559
5	2	4	0.0282	0.5013
6	2	8	0.0020	0.0271
7	2	9	0.0040	0.0850
8	3	4	0.0030	0.0472
9	3	6	0.0007	0.0082
10	4	28	0.0001	0.0250
11	5	6	0.0004	0.0043
12	5	8	0.0004	0.0043
13	6	8	0.0011	0.0292
14	7	35	0.0021	0.0200
15	8	9	0.0050	0.0665
16	9	10	0.0018	0.0213
17	9	11	0.0016	0.0195
18	9	13	0.0008	0.0135
19	9	15	0.0003	0.0800
20	9	18	0.0033	0.0450
21	10	18	0.0033	0.0414

22	13	14	0.0014	0.0500
23	14	15	0.0050	0.2000
24	16	17	0.0032	0.0650
25	17	18	0.0014	0.0147
26	17	19	0.0043	0.0474
27	17	20	0.0057	0.0625
28	19	20	0.0014	0.0300
29	25	29	0.0014	0.0024
30	26	31	0.0016	0.0100
31	27	33	0.0018	0.0100

Table A.3 Generator capacity and dispatch

Generator	Bus No.	MVA Rating	Dispatched P (MW)	V_{Sched} (p.u.)
G01	21	700	Slack	1.0200
G02	22	800	750	1.0300
G03	23	800	800	1.0400
G04	24	1000	850	1.0500
G05	28	2000	1200	1.0400
G06 (WTG)	30	1165	1050	1.0300
G07 (WTG)	32	1065	960	1.0300
G08 (WTG)	34	933	840	1.0250
G09 (WTG)	36	800	720	1.0300

Table A.4 Load data

Load	Bus No.	P (MW)	Q (MVAR)
L01	1	322.0	2.4
L02	2	852.6	220.5
L03	3	565.3	247.8
L04	4	117.9	34.2
L05	6	7.5	44.6
L06	8	54.7	69.8

L07	9	572.8	154.4
L08	10	158.0	30.0
L09	12	628.0	103.0
L10	13	274.0	115.0
L11	14	247.5	84.6
L12	15	308.6	-92.2
L13	16	224.0	47.2
L14	17	139.0	17.0
L15	18	281.0	75.5
L16	19	206.0	27.6
L17	20	283.5	26.9
L18	21	9.2	4.6
L19	28	1104.0	250.0

Table A.5 Data of transformers

Name	S (MVA)	From Bus	To Bus	HV (kV)	LV (kV)	R (p.u.)	X (p.u.)
T01	700	3	21	345	16.5	0.0000	0.1750
T02	800	5	22	345	16.5	0.0000	0.1600
T03	800	7	15	345	16.5	0.0000	0.0909
T04	300	11	12	345	230	0.0007	0.1380
T05	800	11	23	345	16.5	0.0000	0.1190
T06	1000	12	24	345	16.5	0.0080	0.1560
T07	700	14	25	345	16.5	0.0005	0.0272
T08	700	16	26	345	16.5	0.0006	0.2320
T09	1000	20	27	345	16.5	0.0000	0.0909
T10	100	29	30	16.5	0.69	0.0006	0.0047
T11	100	31	32	16.5	0.69	0.0007	0.0051
T12	100	33	34	16.5	0.69	0.0007	0.0060
T13	100	35	36	16.5	0.69	0.0009	0.0068

Appendix B: Link of Publication Included in This Thesis

(1) S. Uddin Mahmud, Nahid-Al-Masood and S. Rahman Deeba, "Assessing Impact on System Strength Under High Wind Power Penetration," *2019 IEEE International Conference on Power, Electrical, and Electronics and Industrial Applications (PEEIACON)*, Dhaka, Bangladesh, 2019, pp. 79-82.
Link: https://ieeexplore.ieee.org/document/9071928